Energy 261 (2022) 125219

Contents lists available at ScienceDirect

Energy

journal homepage: www.elsevier.com/locate/energy

Modelling and analysis of offshore energy hubs

Hongyu Zhang [a,*], Asgeir Tomasgard [a], Brage Rugstad Knudsen [b], Harald G. Svendsen [b], Steffen J. Bakker [a], Ignacio E. Grossmann [c]

[a] Department of Industrial Economics and Technology Management, Norwegian University of Science and Technology, Høgskoleringen 1, 7491, Trondheim, Norway
[b] SINTEF Energy Research, Kolbjørn Hejes vei 1B, 7491, Trondheim, Norway
[c] Department of Chemical Engineering, Carnegie Mellon University, 5000 Forbes Avenue, Pittsburgh, PA 15213, USA

ARTICLE INFO

Keywords:
Clean offshore energy hub
Sensitivity analysis
Deterministic mixed-integer linear programming model

ABSTRACT

Clean offshore energy hubs may become pivotal for efficient offshore wind power generation and distribution. In addition, offshore energy hubs may provide decarbonised energy supply for maritime transport, oil and gas recovery, and offshore farming, while also enabling conversion and storage of liquefied decarbonised energy carriers for export. In this paper, the role of offshore energy hubs is investigated in the transition of an offshore energy system towards zero-emission energy supply. A mixed-integer linear programming model is developed for investment planning and operational optimisation to achieve decarbonisation at minimum cost. We consider offshore wind, solar, energy hubs and subsea cables. A sensitivity analysis is conducted on CO_2 tax, CO_2 budget and the capacity of power from shore. The results show that: (a) a hard carbon cap is necessary for stimulating a zero-emission offshore energy system, (b) offshore wind integration and power from shore can more than halve current emissions, but offshore energy hubs with storage may be necessary for zero-emission production, and (c) at certain CO_2 tax levels, the system with offshore energy hubs can potentially reduce CO_2 emissions by 49% and energy losses by 10%, compared to a system with only offshore renewables, gas turbines and power from shore.

1. Introduction

Offshore wind is an important pillar in the energy transition worldwide [1] to meet global and regional climate targets [2]. Offshore Energy Hubs (OEHs) and the hub-and-spoke concept, offer a transnational and cross-sector solution for better harnessing offshore wind and integration with the rest of the energy system [3]. An energy hub is a physical energy connection point with energy storage where multiple energy carriers can be converted and conditioned [4]. This paper presents an optimisation model for the investment and operation of OEHs. It includes analyses on the functioning of OEHs in the transition of a large-scale energy system towards integrating more renewable energy. A case study is demonstrated in the North Sea as this region has huge potential for large-scale offshore wind [5] and hydrogen production.

The energy transition is widely studied [6]. It includes research on the usage of both renewable energy technologies [7] and energy-efficient technologies [8]. Transitioning to renewable energy, such as, wind, solar, and green hydrogen [9], is a necessity for the decarbonisation of energy systems [10]. Green hydrogen produced from wind and solar power may play an essential role in the transition. Offshore regions with potentially abundant renewable energy sources are crucial for the global energy transition [11]. Therefore, we analyse the potential value of offshore renewable technologies for the energy transition of a regional offshore energy system and discuss how the study can be applied globally to contribute to the global energy transition towards zero emission.

Existing literature reviewed below shows that OEHs may be a promising option for producing green hydrogen offshore. The efficiency and cost analysis of OEHs has shown that an OEH is efficient and cost worthy in electrofuel applications [12]. However, the energy loss of a system with OEHs has not been considered. In this paper, we aim to analyse the potential value of OEHs in terms of energy losses. Producing green hydrogen offshore with OEHs and using the hub generated electricity to firstly cover the nominal electrolyser capacity may be cost competitive compared with current costs of grey and blue hydrogen [13]. The energy storage function of OEHs has not been considered, which makes their OEH essentially a conversion and distribution hub. Offshore energy storage can be crucial because of the

Abbreviations: NCS, Norwegian continental shelf; OEH, Offshore energy hub; PFS, Power from shore; Base, The case with only offshore renewables, gas turbines and power from shore; S1, Scenario 1; S2, Scenario 2; MILP, Mixed-integer linear programming

* Corresponding author.
E-mail address: hongyu.zhang@ntnu.no (H. Zhang).

https://doi.org/10.1016/j.energy.2022.125219
Received 12 October 2021; Received in revised form 24 June 2022; Accepted 18 August 2022
Available online 24 August 2022

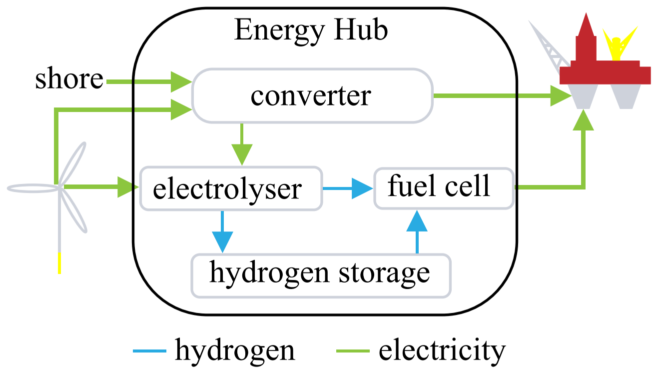

Fig. 1. Conceptual illustration of OEHs.

potential massive capacity [14]. Therefore, in this paper, we consider OEHs with offshore hydrogen storage, see Fig. 1 for an illustration.

In addition to distributing offshore energy to onshore systems with OEHs, existing literature also investigates using OEHs for decarbonised energy supply for offshore industries [15], including offshore oil and gas recovery [16], maritime cargo transport, and offshore farming [17]. The environmental value of OEHs has not been analysed in the literature. Cost estimation of electrifying offshore fields with OEHs is presented in [18]. However, the costs data was not used for investment planning to analyse the trade off of technologies. The value of OEHs for offshore sectors on a large scale is not sufficiently studied. Although green hydrogen is pointed out as promising storage that can provide supply security for oil and gas operations, it was not analysed.

To bridge the gaps mentioned above, we develop a multi-carrier Mixed-Integer Linear Programming (MILP) model for investment planning optimisation of an offshore energy system with a high degree of operational details. We model a clean OEH with hydrogen storage. We only consider producing green hydrogen from electrolysis. To analyse the economic advantages of OEHs compared with other technologies, we consider investments in offshore wind, offshore solar, OEHs and Power From Shore (PFS). The investment planning model is applied to an offshore energy system with the goal of decarbonising energy generation for offshore oil and gas installations in a given region. The oil and gas industry involves multi-billion-dollar investments and profits [19] whose decarbonisation needs may trigger large-scale investments in OEHs. Offshore oil and gas is an important offshore sector in many countries, and the North Sea region has the highest number of offshore fields [20]. Therefore, studying the value of clean OEHs in the North Sea energy system may provide global insights.

The contributions of the paper are: (1) an integrated investment and operational model with the following features, (a) OEHs are modelled for a large-scale offshore energy system, and (b) the hourly device-level energy consumption of platforms is modelled; (2) the value of OEHs is analysed in the North Sea offshore energy system transition towards zero-emission energy supply.

The outline of the paper is as follows: Section 2 presents a literature review on energy system planning methods and OEHs and introduces the background regarding the production and decarbonisation of offshore oil and gas. Section 3 gives the problem description followed by modelling strategies and assumptions. Section 4 presents the MILP model and the case study. Section 5 describes the case study and input data. Section 6 presents the results and analysis of the case study. Section 7 discusses the implications of the results and summaries the limitations of the research. Section 8 concludes the paper and suggests further research.

2. Literature review

In this section, we review the literature on energy system planning methods and OEHs and give a background on the production process of offshore fields and corresponding decarbonisation issues.

2.1. Energy system planning methods

From an energy system planning perspective, the model in this paper is a bottom-up multi-carrier energy flow model. For an extensive review on this topic, we refer to [21]. Bottom-up energy system models represent the equilibrium of a part of the energy sector [22]. On the other hand, top-down energy models try to depict the economy as a whole on a national level to analyse the aggregated effects of energy policies in monetary units. In this paper, we only use the bottom-up approach without considering the effect from a higher level using a soft-link or hard-link model because we are interested in the cost-optimal system design under different policy and technical scenarios rather than analysing its interaction with the macro economy.

For large-scale energy system planning problems, linear programming (LP) is usually used because of its computational tractability and sufficiency in modelling most investment and operational decisions and constraints. For example, energy system planning models like EMPIRE [23], and GENeSYS-MOD [24] are LP models. Even though LP may be sufficient when dealing with very aggregated systems, for problems with lumpy investments (e.g. OEHs or transmission lines), LP cannot capture the economic scale of the investment decision, and MILP models are preferred [25]. Mixed-integer nonlinear programming is also used in a planning problem to capture the system operations [26]. However, the computational difficulty may need to be addressed first to make the problem solvable. Our model uses MILP to provide more sensible investment decisions and avoid nonlinear constraints by simplifying the problem to reduce computational costs.

2.2. OEHs

The potential value and functioning of OEHs have drawn increased attention in several sectors. In the offshore oil and gas sector, it has been found that creating small energy hubs to import energy from various sources to offshore oil and gas platforms can achieve a massive reduction of CO_2 emissions in the UK continental shelf [18]. They mentioned that hydrogen-energy storage is green and provides supply security for oil and gas operations. Energy-hub-based electricity system design for an offshore platform considering CO_2 mitigation is presented in [16]. By verifying the proposed approach on an existing platform, it was found that CO_2 tax may play a decisive role in emission mitigation of offshore platforms. In addition to clean OEHs that utilise offshore wind, an OEH equipped with large gas turbines was proposed in [27]. Such an OEH serves as a centralised power generation system that offers higher efficiencies than simpler in situ gas turbines [27].

OEHs may allow for better harnessing offshore wind to supply more stable energy to offshore oil and gas platforms in the short run and export clean energy to the continent in the long run. Connecting offshore wind in the North Sea, via an artificial island and hub-and-spoke form, was shown in [28] to be more economical than a traditional point-to-point connection if 10 GW offshore wind is built. Hydrogen based OEHs also draw attention. An offshore artificial power-to-gas island can produce and transport hydrogen through natural gas pipelines [29]. Adding electrolysers to the offshore hub shows value in mitigating active power variations and maintaining the voltage of the hub [30]. Producing green hydrogen via OEHs to cover onshore energy demand and using hub generated electricity first to cover nominal electrolyser capacity may have better economic performance than producing hydrogen from natural gas [13]. In addition, techno-economic analysis of offshore energy islands has shown that producing hydrogen offshore may be more beneficial than onshore production under some conditions. However, the development of offshore energy islands for electrical transmission and hydrogen production is not straightforward [31].

Studies have also been conducted on the impact of markets and the design of markets in a system with OEHs. The impact of the North Sea energy islands on national markets and grids is analysed

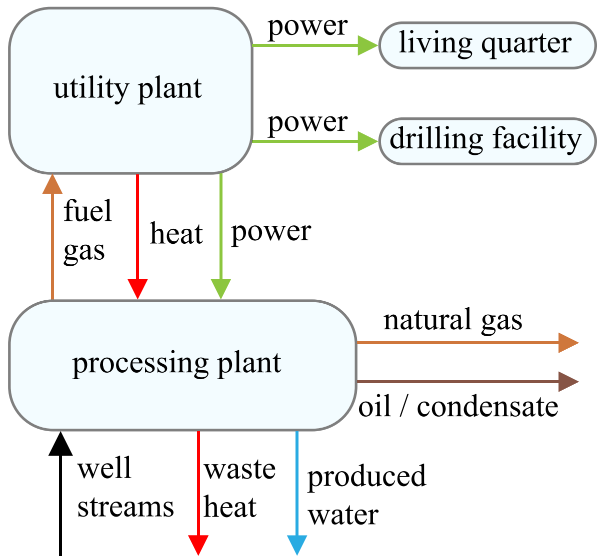

Fig. 2. Schematic of a topside structure of a typical North Sea oil and gas platform. *Source:* Adapted from [46].

in [32] using a European electricity market model and a European electricity network model, where the authors found that social welfare increases but not for all the countries when the North Sea energy hub is included in the system. Moreover, a separate offshore bidding zone may lead to a more efficient offshore energy system with OEHs [33]. We consider a smaller system and focus on the optimal capacities of new devices instead of analysing an extensive grid based on the assumption that a certain amount of capacity of an OEH will be added. The deployment plan for future European offshore grid development with an energy hub is analysed in [34]. Unlike the study in this paper, they assume some scenarios of future deployment of wind turbines and transmission lines and analyse the system operation under different operational scenarios, including line fault, breaker failure, and bus bar fault. Compared with our study, they focus more on system operation under a predefined system configuration. We notice that in the study mentioned above, where the focus is on national markets, grid, and system failure, the investment planning and operations of OEHs are simplified. Therefore, we aim to contribute to more detailed modelling of optimising investment planning and operation of OEHs.

In addition to OEHs, more research has been conducted on the onshore energy system. The energy hub concept has been also used to increase the energy flexibility in buildings [35] and electricity markets [36]. Energy hub is a promising option for exploiting the benefits of multi-energy systems, such as coupled electricity and heating networks [37], integrated natural gas and electricity [38] and electricity–thermal–natural gas coupling system [39]. In addition, the design [40] and management [41] of energy hubs with penetration of intermittent wind power has been studied using stochastic programming. Using energy hubs for coping with wind power volatility shows value in reducing operating cost, wind power curtailment and CO_2 emissions [42]. Energy hubs with power-to-gas and hydrogen storage can reduce emissions, and produce hydrogen for end-use applications [43]. Onshore energy hubs have much more versatile configurations and functioning compared to OEHs. We refer the readers to [44,45] for comprehensive reviews on the research works on energy hubs.

2.3. Offshore oil and gas fields

From the studies on offshore field production optimisation [47] and offshore field infrastructure planning [48], we can see that platforms and fields vary a lot due to, amongst others, geological characteristics, reserves, and remaining lifetimes. In the following, we present a typical composition and production process of NCS platforms.

A North Sea field normally consists of topside structures and subsea production systems. A topside structure typically consists of a processing plant, a utility plant, drilling facilities, and a living quarter [46], see Fig. 2. The production plant receives and processes well streams. A visualisation of the production process is presented in Fig. 3. Major energy consumption takes place in the production plants. The energy demand of production plants is conventionally fulfilled by gas turbines located in the utility plant. In 2014, gas turbines with waste heat recovery units covered approximately 90% of all heat demand for operations on the NCS [49].

2.4. Decarbonisation of offshore fields

Norway was the world's third-largest exporter of natural gas in 2019 [50]. Offshore oil and gas extraction was responsible for 26.6% (13.3 Mt CO_2 equivalent) of the total Norwegian greenhouse gases in 2020 [51]. Norway steps up its climate goal to reduce emissions by 50%–55% by 2030 compared to 1990 levels [52]. Using OEHs to effectively exploit offshore wind power to decarbonise the NCS energy system may contribute to meeting Norway's and Europe's climate targets.

CO_2 tax is an important instrument for stimulating offshore energy system decarbonisation. In 2022, the tax is about 79 €/tonne in Norway [53] with an ambition to increase it to 200 €/tonne by 2030 [54]. In addition, the EU Emissions Trading System is a "cap and trade" system that also includes the emissions on the NCS [54]. Carbon tax and the emissions trading system make a total carbon price of approximately 160 €/tonne. In this context, oil and gas companies are undertaking considerable investments in decarbonisation solutions to address climate goals, such as PFS and offshore wind. Oil and gas companies on the NCS have set climate targets. For example, Equinor [55] and Vår Energy [56] aim to reduce greenhouse gas emissions by 40% by 2030, and near zero emission by 2050.

Technologies for decarbonisation exist, and the question is to find the best mixture of such technologies at acceptable costs. There are four general approaches to reduce offshore CO_2 emissions, when maintaining a certain activity level:

(a) Reducing CO_2 emissions by improving reservoir drainage and processing energy efficiency [57]. Water injection and gas injection are common reservoir drainage strategies used on the NCS. Pumping, compression and separation are major processes for handling produced fluids and gas in a processing system. Injection and processing account for more than half of the power consumption at the fields on the NCS.

(b) Increasing the energy efficiency of gas turbines. Due to security of supply requirements, gas turbines usually operate with a margin, which leads to a low efficiency of around 33% [58]. Adding bottoming cycles to the existing gas turbines can improve their energy efficiency. However, unlike an onshore energy system, weight and space limitation of an offshore installation restrict extra devices like a bottoming cycle.

(c) Supplying zero emission or low emission energy to offshore oil and gas platforms. This includes PFS [59], switching fuel from natural gas to ammonia or hydrogen, and connecting offshore wind farms to platforms. In the past years, several offshore fields have received PFS via HVDC/HVAC cables [60]. In Norway, the cost of abating CO_2 emissions by taking PFS can vary from less than 100 to almost 800 €/tonne [61]. Many abatement projects bringing PFS, are in their planning phase highly unprofitable even considering Norway's plan to increase CO_2 tax to 200 €/tonne in 2030. Besides, due to the capacity limits of the onshore system, the available power is limited in some cases.

Offshore wind is another technology to supply clean power to platforms. Equinor's Hywind Tampen project aims to be operational by 2022 [62]. The combination of an offshore platform with a wind farm represents a potentially good match for the offshore petroleum sector's

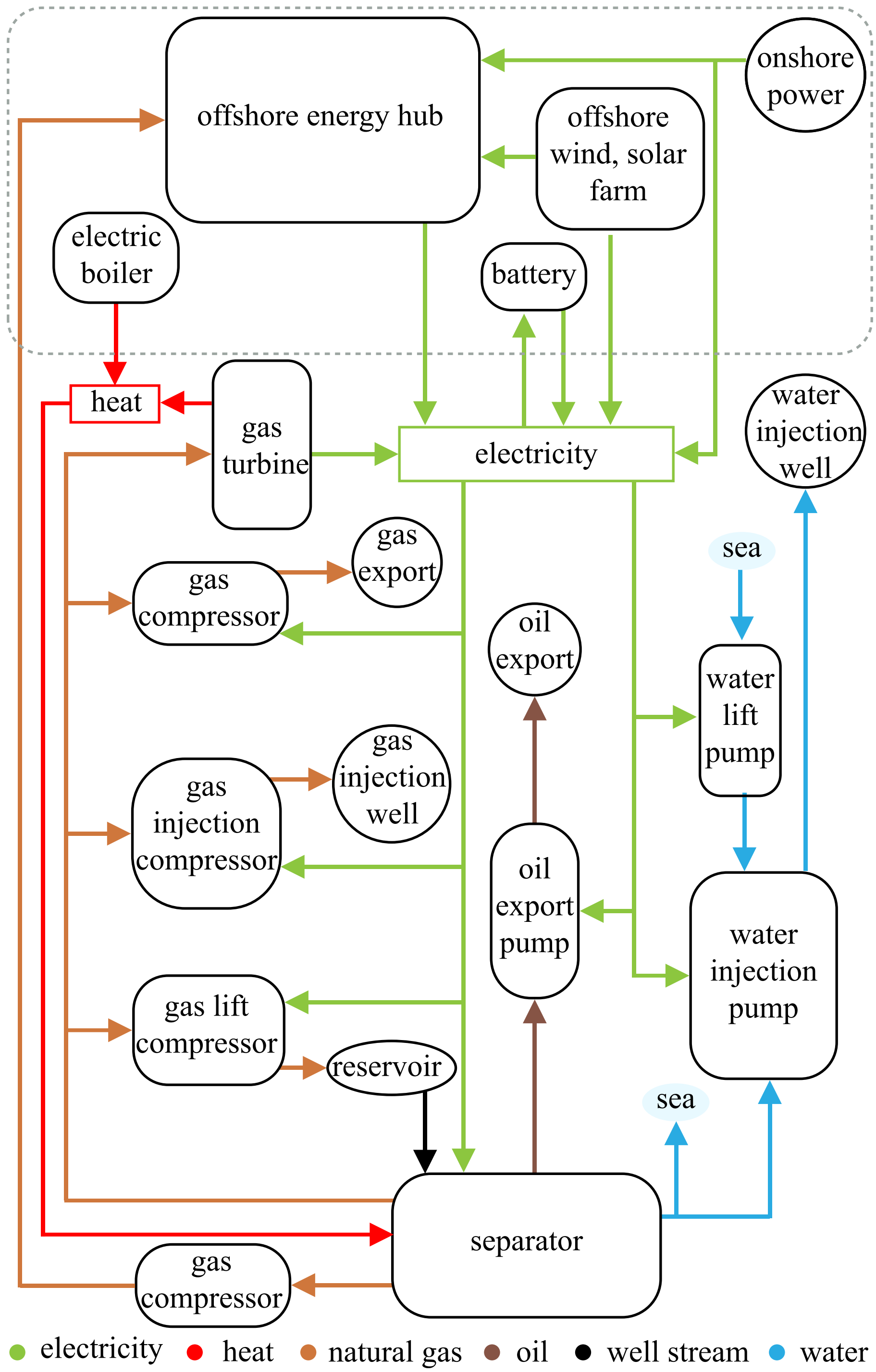

Fig. 3. Schematic of a potential decarbonised offshore field production process. A three-stage separator train separates well streams into produced water, oil, condensate and gas. Typically the first stage separator takes out most of the water and gas at arrival conditions. Fuel gas is taken from the first stage separator. The residual mix of oil, gas and water is heated before entering the second stage separator. Produced water is purified and discharged, and in some cases, reinjected into water injection wells to maintain reservoir pressure. Water lift pumps will lift seawater for reinjection if needed. Produced oil is pressurised by pumps and exported. Produced gas is used as fuel gas, compressed and exported, reinjected via dedicated wells for enhanced oil recovery or injected into the same wells for gas lift.
The grey dotted box includes the potential processes for decarbonisation. See Fig. 1 for a visualisation of the processes in an OEH.

desire for renewable energy with the offshore wind power industry's desire for an early market [63]. The stability and control issues for an isolated offshore energy system consisting of a wind farm and five platforms were addressed in [63]. Integrating large wind turbines into a stand-alone platform is theoretically possible, but requires more operational and economic work to prove its feasibility [64]. In [65], authors found that local wind power production for matching the offshore power demand improves both voltage- and frequency-stability in an offshore system. An MILP model for determining optimal offshore grid structures for wind power integration and power exchange named Net-Op was presented in [66]. An extension of Net-Op that takes into account investment cost, variability of wind/demand/power prices, and the benefit of power trade between countries/price areas is presented in [67].

(d) Deploying carbon capture and storage. Storing CO_2 in stable underground formations, e.g., old and stable oil reservoirs, has a relatively long history. Since 1996, nearly one million tonnes of CO_2 per year have been separated during the natural gas process from the Sleipner Vest field and stored in the Utsira formation [59].

The first two approaches have a limited impact on emission reduction, whereas the third and fourth approaches can give up to 100% reduction. We focus on supplying clean energy to offshore fields.

3. Problem description

First, this section introduces the proposed offshore energy system planning problem with OEHs. Then, we present the time and geographical structures with the aim of reducing computational time of a potentially large problem. Finally, we state the modelling assumptions.

The problem under consideration aims to make optimal investment and operational decisions for the NCS energy system with OEHs, based on the energy demand captured by the operational model. By solving such a problem, we aim to find out under what conditions OEHs may benefit the system and how OEHs operate with the rest of the system.

To model hourly energy demand, the following devices are considered: (a) separators; (b) pumps: water injection pumps, water lift pumps, oil export pumps; (c) compressors: gas injection compressors and gas export compressors. These devices have existing capacities, and no investment is made in them. Moreover, we assume that device efficiency, flow inlet/outlet pressures and hourly mass flow are given.

For the investments in decarbonisation solutions, we consider: (a) offshore renewable energies (offshore wind and offshore solar); (b) OEHs (electrolysers, hydrogen storage facilities and fuel cells); (c) subsea cables (HVAC, HVDC and offshore and onshore converter stations); (d) electric boilers; (e) platform located batteries. The capital expenditures, fixed operational costs are assumed to be known.

The problem is to determine: (a) capacities of decarbonisation technologies, and (b) operational strategies that include scheduling of generators, storage and approximate power flow among regions to meet the energy demand with minimum overall investment, operational and environmental costs.

3.1. Modelling strategies and assumptions

A multilevel control hierarchy was defined in [68], arguing that the repetitive use of static models can solve many important petroleum production optimisation problems. A multi-period MILP model is developed for an integrated investment planning and operational problem that combines short-term and long-term control hierarchies. Aggregation, clustering and time sampling [69] are used to address the multi-time-scale aspects [70] and solve a large-scale instance.

3.1.1. Time structure of the problem

The investment problem is optimised over a long-term horizon, e.g., a few decades. The operational problem is optimised on an hourly basis based on investment decisions. To combine these two control hierarchies without increasing much the computational time, N representative slices are selected, each containing h hours, and they are scaled up to represent a whole operational year. A visualisation of the time structure is in Fig. 4.

We use a node formulation to link investment planning with the system operation. An illustration of a planning problem is presented in Fig. 5. We define a point in time where investments are made as an investment node i_0. We then define the entire operational problem succeeding an investment node as an operational node i. Finally, the investment decision made in an investment node is examined by the operational node succeeding the investment node.

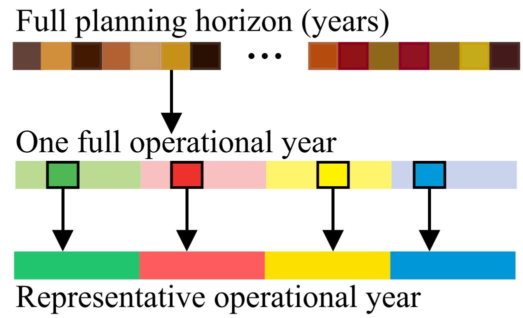

Fig. 4. Illustration of combined hierarchies.
Source: Adapted from [71].

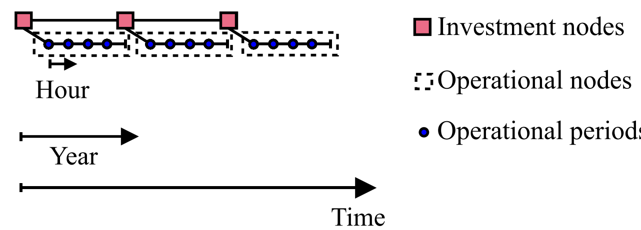

Fig. 5. Illustration of the linkage between investment planning and operational time horizon.

3.1.2. Geographical structure of the problem

The problem potentially consists of many regions, and we implement a k-means cluster method based on the locations of fields to reduce the problem size. There are two considerations when deciding the number of clusters. Firstly, we assume the OEH connects the surrounding fields via HVAC cables; thus, only fields with a feasible transmission distance (up to 100 km) are considered. Secondly, we assume that the cluster centres are the locations for OEHs. We prevent clusters with too few fields. For each cluster, we aggregate the individual fields into one larger field with a distance to the OEH equal to the average distance of the individual fields, and connect fields to OEH in hub-and-spoke form. Currently, we do not consider the interconnection among fields and clusters, resulting in reasonably simple network topology.

3.1.3. Assumptions

Each platform is assumed to be a typical North Sea platform with production processes as shown in Fig. 3. The energy consumption of pumps, compressors and separators can be formulated as a function of flow rate, pressure and temperature. For simplicity, the pressure levels and temperatures are assumed to take values that are typical on the North Sea, leading to a linear formulation. Kirchhoff voltage law is omitted, and replaced by an energy flow model. We assume no mass loss during production.

4. Mathematical model

This section presents a deterministic MILP formulated for the multi-carrier energy system investment planning problem with high degree of operational details. The model includes a long-term investment planning horizon and a short-term operational horizon. The integrated investment planning and operational model is partially based upon the linear programming model developed in [72]. Integer variables are used to improve the representation of the fixed capacity independent investment costs. The complete MILP problem consists of Eqs. (1)–(3).

The complete nomenclature of the model can be found in Appendix A. The supplementary definitions of some model parameters are presented in Appendix C. We use the conventions that calligraphic capitalised Roman letters denote sets, upper case Roman and lower case Greek letters denote parameters, and lower case Roman letters denote variables. The indices are subscripts and name extensions are superscripts. The same lead symbol represent the same type of thing. The names of variables, parameters, sets and indices are single symbols.

4.1. Objective function

$$\min c^{INV} + \kappa \sum_{i\in\mathcal{I}} c_i^{OPE} \tag{1}$$

The objective function, Eq. (1), is to minimise the total investment (c^{INV}) and operational ($\kappa \sum_{i\in\mathcal{I}} c_i^{OPE}$) costs over the planning horizon.

4.2. Investment planning constraints

The investment planning constraints are given by:

$$c^{INV} = \sum_{i\in\mathcal{I}_0}\sum_{p\in\mathcal{P}} \left(C_{pi}^{InvV} x_{pi}^{Inst} + C_{pi}^{InvF} y_{pi} \right) + \kappa \sum_{i\in\mathcal{I}}\sum_{p\in\mathcal{P}} C_{pi}^{Fix} x_{pi}^{Acc} \tag{2a}$$

$$x_{pi}^{Acc} = X_p^{Hist} + \sum_{i\in\mathcal{I}_i} x_{pi}^{Inst}, \qquad p\in\mathcal{P}, i\in\mathcal{I} \tag{2b}$$

$$0 \le x_{pi}^{Inst} \le Q_p y_{pi}, \qquad p\in\mathcal{P}, i\in\mathcal{I}_0 \tag{2c}$$

$$0 \le x_{pi}^{Acc} \le X_p^{Max}, \qquad p\in\mathcal{P}, i\in\mathcal{I} \tag{2d}$$

$$y_{pi} \in \{0,1,2,\dots,Y_{pi}\}, \qquad p\in\mathcal{P}, i\in\mathcal{I}_0 \tag{2e}$$

$$x_{pi}^{Inst}, x_{pi}^{Acc} \in \mathbb{R}_0^+, \tag{2f}$$

$$y_{pi} \in \mathbb{Z}_0^+. \tag{2g}$$

The total cost for investment planning, Eq. (2a), consists of actual investment costs (comprising capacity-dependent and capacity-independent costs), as well as fixed operating and maintenance costs. Here, κ is a scaling factor that depends on the time step between two successive investment nodes. Constraint (2b) states that the accumulated capacity of a technology x_{pi}^{Acc} in an operational node equals the sum of the historical capacity X_p^{Hist} and newly invested capacities x_{pi}^{Inst} in its ancestor investment nodes $\mathcal{I}_i$. The integer variable y_{pi} gives the number of units of technology $p\in\mathcal{P}$ in investment node $i\in\mathcal{I}_0$. Parameter Q_p represents the maximum capacity of a technology unit, and parameter X_p^{Max} denotes the maximum accumulated capacity of a technology. Parameter Y_p gives the maximum number of units that can be installed for the different technologies.

4.3. Operational constraints

We now present the operational constraints in one operational node i. Note that we omit index i in the operational model for ease of notation. Oil and gas recovery are modelled as this is the most likely use in the short to medium term. The operational constraints can be modified for other use, e.g., offshore fish farming, maritime, transport, and others.

$$c^{OPE} = \sum_{t\in\mathcal{T}_n} W_t \left(\sum_{g\in\mathcal{G}} C_g^G p_{gt}^G + \sum_{z\in\mathcal{Z}}\sum_{l\in\{H,P\}} C^{Shed,l} p_{zt}^{Shed,l} + \sum_{z\in\mathcal{Z}^O} \tau_{zt}^{EP} p_{zt}^{PFS} \right) \tag{3a}$$

$$0 \le p_{pt} \le p_p^{Acc}, \qquad p\in\mathcal{P}^*, t\in\mathcal{T} \tag{3b}$$

$$0 \le p_{gt}^G + p_{gt}^{ResG} \le p_g^{AccG}, \qquad g\in\mathcal{G}, t\in\mathcal{T} \tag{3c}$$

$$0 \le v_{st}^{SHy} \le v_s^{AccSHy}, \qquad s\in\mathcal{S}^{Hy}, t\in\mathcal{T} \tag{3d}$$

$$0 \le p_{st}^{SE+} \le \gamma_s^{SE} q_s^{AccSE}, \qquad s\in\mathcal{S}^E, t\in\mathcal{T} \tag{3e}$$

$$0 \le p_{st}^{SE-} + p_{st}^{ResSE} \le \gamma_s^{SE} q_s^{AccSE}, \qquad s\in\mathcal{S}^E, t\in\mathcal{T} \tag{3f}$$

$$0 \le q_{st}^{SE} \le q_s^{AccSE}, \qquad s\in\mathcal{S}^E, t\in\mathcal{T} \tag{3g}$$

$$-p_l^{AccL} \le p_{lt}^L \le p_l^{AccL}, \qquad l\in\mathcal{L}, t\in\mathcal{T} \tag{3h}$$

$$-\alpha_g^G p_g^{AccG} \le p_{gt}^G + p_{gt}^{ResG} - p_{g(t-1)}^G - p_{g(t-1)}^{ResG} \le \alpha_g^G p_g^{AccG}, \qquad g\in\mathcal{G}, n\in\mathcal{N}, t\in\mathcal{T}_n \tag{3i}$$

$$-\alpha_f^F p_f^{AccF} \le p_{ft}^F - p_{f(t-1)}^F \le \alpha_f^F p_f^{AccF}, \qquad f\in\mathcal{F}, n\in\mathcal{N}, t\in\mathcal{T}_n \tag{3j}$$

$$\sum_{g\in\mathcal{G}_z} p_{gt}^{ResG} + \sum_{s\in\mathcal{S}_z^E} p_{st}^{ResSE} \ge \sigma_z^{Res} P_{zt}^{DP}, \qquad z\in\mathcal{Z}^P, t\in\mathcal{T} \tag{3k}$$

$$\sum_{g\in\mathcal{G}_z} p_{gt}^G + \sum_{l\in\mathcal{L}_z^{In}} \eta_l^L p_{lt}^L + \sum_{s\in\mathcal{S}_z^E} p_{st}^{SE-} + \sum_{r\in\mathcal{R}_z} R_{zt}^R p_r^{AccR} + \sum_{f\in\mathcal{F}_z} p_{ft}^F + p_{zt}^{ZO} + p_{zt}^{ShedP} = P_{zt}^{DP} + \sum_{b\in\mathcal{B}_z^E} p_{bt}^{BE} + \sum_{e\in\mathcal{E}_z} p_{et}^E + \sum_{l\in\mathcal{L}_z^{Out}} \eta_l^L p_{lt}^L + \sum_{s\in\mathcal{S}_z^E} p_{st}^{SE+} + p_{zt}^{GShedP}, \qquad z\in\mathcal{Z}, t\in\mathcal{T} \tag{3l}$$

$$\sum_{g\in\mathcal{G}_z} \eta_g^{HrG} p_{gt}^G + \sum_{b\in\mathcal{B}_z^E} \eta_b^{BE} p_{bt}^{BE} + p_{zt}^{ShedH} = P_{zt}^{DH} + p_{zt}^{GShedH}, \qquad z\in\mathcal{Z}^P, t\in\mathcal{T} \tag{3m}$$

$$\eta^{EF}\Big(\sum_{f\in\mathcal{F}_z} H_t \rho^F p_{ft}^F - \sum_{s\in\mathcal{S}_z^{Hy}} v_{st}^{SHy-}\Big) = \sum_{e\in\mathcal{E}_z} H_t p_{et}^E - \eta^{ES} \sum_{s\in\mathcal{S}_z^{Hy}} v_{st}^{SHy+}, \qquad z\in\mathcal{Z}^H, t\in\mathcal{T} \tag{3n}$$

$$H_t(p_{st}^{ResSE} + p_{st}^{SE-}) \le q_{st}^{SE}, \qquad s\in\mathcal{S}^E, t\in\mathcal{T} \tag{3o}$$

$$q_{s(t+1)}^{SE} = q_{st}^{SE} + H_t(\eta_s^{SE} p_{st}^{SE+} - p_{st}^{SE-}), \qquad s\in\mathcal{S}^E, n\in\mathcal{N}, t\in\mathcal{T}_n \tag{3p}$$

$$v_{s(t+1)}^{SHy} = v_{st}^{SHy} + v_{st}^{SHy+} - v_{st}^{SHy-}, \qquad s\in\mathcal{S}^{Hy}, n\in\mathcal{N}, t\in\mathcal{T}_n \tag{3q}$$

$$\sum_{t\in\mathcal{T}_n}\sum_{g\in\mathcal{G}} W_t E_g^G p_{gt}^G \le \mu^E, \tag{3r}$$

$$p_{lt}^L \in \mathbb{R}, \quad p_{gt}^G, p^{ShedP}, p^{ShedH}, p_{zt}^{PFS}, p_{pt}, p_p^{Acc}, p_{gt}^G, p_{bt}^{BE} \in \mathbb{R}_0^+, \tag{3s}$$

$$p_{gt}^{ResG}, p_g^{AccG}, p_{zt}^{GShedP}, p_{zt}^{GShedH}, v_{st}^{SHy+}, v_{st}^{SHy-}, v_{st}^{SHy}, p_{et}^E \in \mathbb{R}_0^+, \tag{3t}$$

$$v^{AccSHy}, p_{st}^{SE+}, p_{st}^{SE-}, p_{st}^{ResSE}, q_s^{AccSE}, q_{st}^{SE}, p_l^{AccL}, p_r^{AccR}, p_{ft}^F \in \mathbb{R}_0^+. \tag{3u}$$

The operational cost c^{OPE}, which is included in the objective function, Eq. (1), for each operational node i, is described by Eq. (3a) that includes total operating costs of generators $C_g^G p_{gt}^G$, energy load shedding costs for heat $C^{ShedH} p^{ShedH}$ and power $C^{ShedP} p^{ShedP}$ and electricity costs of onshore power $\tau_{zt}^{EP} p_{zt}^{PFS}$. C_g^G includes the variable operational cost, fuel cost and the CO_2 tax charged on the emissions of generator g. Constraint (3b) ensures that the devices including electric boilers $b\in\mathcal{B}^E$, electrolysers $e\in\mathcal{E}$, and fuel cells $f\in\mathcal{F}$ are within their capacity limits. Constraint (3c) dictates that the power generation of a gas turbine p_{gt}^G plus the spinning reserve p_{gt}^{ResG} must not exceed its capacity p_g^{AccG}. Constraint (3d) states that the hydrogen storage level v_{st}^{SHy} should be less than the capacity v_s^{AccSHy}. Constraint (3e) dictates that the power charged p_{st}^{SE+} should be within the charging capacity. Constraint (3f) specifies that the discharging power p_{st}^{SE-} plus the power for reserve requirement p_{st}^{ResSE} must not exceed the discharging capacity. Constraint (3g) limits the energy storage level q_{st}^{SE} to be within the capacity q_s^{AccSE}. Constraint (3h) shows that the power flow p_l^L is within the transmission capacity p_l^{AccL}. Constraints (3i) and (3j) capture how fast gas turbines and fuel cells can ramp up or ramp down their power output, respectively. The parameters α_g^G and α_f^F are the maximum ramp rate of gas turbines and fuel cells, respectively. The operating reserve requirement, Constraint (3k), dictates that the spinning reserve of gas turbines p_{gt}^{ResG}, plus the reserve of the electricity storage p_{st}^{ResES} must exceed the minimum reserve requirement, where σ^{Res} is a percentage of the power load. The power nodal balance, Constraint (3l), ensures that, in one operational period t, the sum of total power generation of turbines p_{gt}^G, power discharged from all the electricity storage p_{st}^{SE-}, renewable generation $R_{zt}^R p_{rt}^{AccR}$, fuel cell generation p_{ft}^F, power transmitted to this region, and load shed

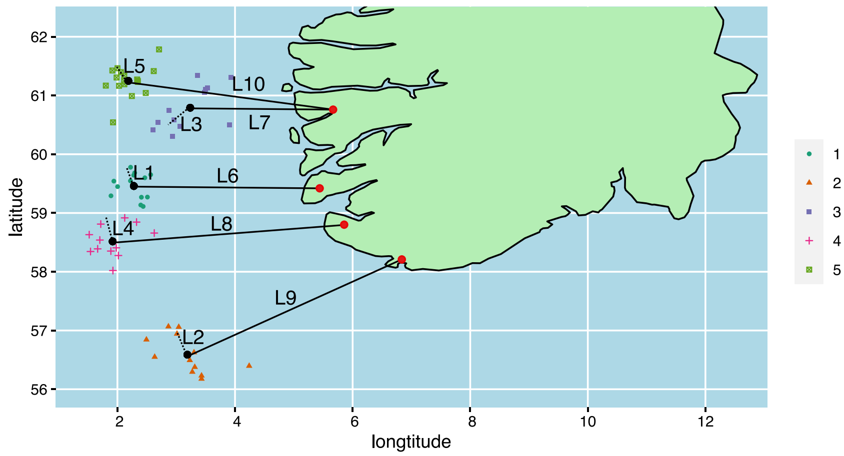

Fig. 6. Illustration of the NCS energy system with energy hubs. L1 – L5 (dotted lines) are representative HVAC cables, while L6 – L10 (solid lines) are HVDC cables. Black dots represent energy hubs and the red dots represent the onshore buses they connect to. Points with different shapes and colours represent NCS oil and gas fields.

p^{ShedP}_{zt} equals the sum of power demand P^{DP}_{zt}, power consumption of electric boilers p^{BE}_{bt}, power consumption of all electrolysers p^{E}_{et}, power transmitted to other regions, and power generation shed p^{GShedP}_{zt}. The parameter R^{R}_{zt} is the capacity factor of renewable unit that is a fraction of the nameplate capacity p^{AccR}. The subset of a technology in region z is represented by $R_z := \{r \in \mathcal{R} : r$ is available in region $z\}$, where $\mathcal{R}$ can be replaced by other sets of technologies. The heat energy balance, Constraint (3m), states that the heat recovery of gas turbines $\eta^{HrG}_{g} p^{G}_{gt}$, plus electric boiler heat generation $\eta^{BE}_{b} p^{BE}_{bt}$, plus heat load shed p^{ShedH}_{zt} equals the heat demand P^{DH}_{zt} plus the heat generation shed p^{GShedH}_{zt}. The hydrogen mass balance, Constraint (3n), states that hydrogen produced by electrolyser equals the hydrogen injected into the storage v^{SHy+}, plus the hydrogen directly supplied to fuel cells . Constraint (3o) restricts the discharged energy and the energy for reserve purpose to be less than the energy storage level q^{SE}_{st}. Constraint (3p) states that the state of charge q^{SE}_{st} in period $t+1$ depends on the previous state of charge q^{SE}_{st}, the charged power p^{SE+}_{st} and discharged power p^{SE-}_{st}. The parameter η^{SE}_{s} represent the charging efficiency. The parameter H_t is the length of the period t. The hydrogen storage balance, Constraint (3n), shows that the hydrogen storage level v^{SHy}_{st} at period $t+1$ equals to storage level at the previous period, plus the hydrogen injected v^{SHy+}_{st}, minus the hydrogen withdrawn v^{SHy-}_{st}. Constraint (3r) restricts the total emission. The parameter μ^{E} is the CO_2 budget. The symbol E^{G}_{g} is the emission factor per unit of power generated. The parameter W_t is the length of a period after scaling. We only consider emissions from the generators, but the model can easily be extended to include other emissions. The complete MILP problem consists of Eqs. (1)–(3).

5. Case study

The case study is carried out on the North Sea part of the NCS, considering 66 fields. The problem consists of 77 regions, divided into 66 fields, 5 OHEs and 5 onshore buses. By using the clustering approach described in Section 3.1, the system can be represented using 5 clusters and henceforth go from 77 regions to 15 regions. The network topology is exemplified in Fig. 6. The power demand of platforms is assumed to be initially entirely supplied by gas turbines, as only a limited number of platforms receives PFS. Four representative months with hourly resolution are selected and scaled up to represent a whole year. In the case study, parameter Q_p is obtained from references. It is determined based on the nameplate capacity of devices. The parameter X^{Max}_{p} is set to a big number.

The field area geometry data is obtained from [73]. For each field, one coordinate is picked from the multipolygon as its representative location. The representative location, attributed cluster and the distance to its cluster centre for each field are summarised in Table D.2.

One month from each season is selected. The production of fields in each cluster is aggregated. A visualisation of the production data for each field in the four representative months is presented in Fig. 7, the data used for plotting is available at [74].

The operational data in the oil and gas industry is sensitive, and usually not disclosed to the public. Aggregated data such as monthly or yearly production of petroleum on the NCS can be obtained from [59]. One can also find monthly production and injection data for each field from [75,76]. Neither of these can be directly used as inputs for this study due to the time resolution difference. Therefore, reasonable data generation is necessary. Raw data is collected from: (a) Norne (1998–2006) and Volve (2008–2016) fields with hourly production and injection data from [77], and (b) monthly production and injection data of each field from [75]. We develop a data generation method that considers the lifetimes of offshore fields [74].

We define a base case (Base) with offshore renewables, electric boiler, battery and PFS as investment options. This case is then used as a benchmark to check against the case with OEHs. The full model given by Eqs. (1)–(3) takes approximately 2 hours to solve.

6. Results

We demonstrate the results of a static integrated investment planning and operational problem given by Eqs. (1)–(3), for a future point in time. The problem consists of 461,208 continuous variables, 100 integer variables and 980,013 constraints. The model was implemented in Julia 1.6.1 using JuMP [78] and solved with Gurobi 9.1.2 [79]. The code was run on a MacBook Pro with 2.4 GHz 8-core Intel Core i9 processor, with 64 GB of RAM, running on macOS 11.6 Big Sur. The Julia code and data for the case study have been made publicly available [74]. The integrated investment and operational model given by Eqs. (1)–(3) is solved to conduct sensitivity analysis on CO_2 tax, CO_2 budget and the capacity of PFS. The results show that a system with OEHs can reduce up to 49% CO_2 emissions and 10% energy loss compared with the one with only offshore renewables, gas turbines and PFS.

6.1. Energy system analysis

In this section, we present results on energy consumption and CO_2 emission of the initial system. By post-processing, we verify the energy consumption of platforms is of the same order of magnitude as the reported numbers. The resulted CO_2 emission is 5.54 Mt/yr. In comparison, the reported total emission of the relevant fields was 6.89 Mt in 2019 [76]. The emissions from the model are expected to be lower than 6.89 Mt since not all emission sources are considered. Based on [80], one could assume that the major processes considered

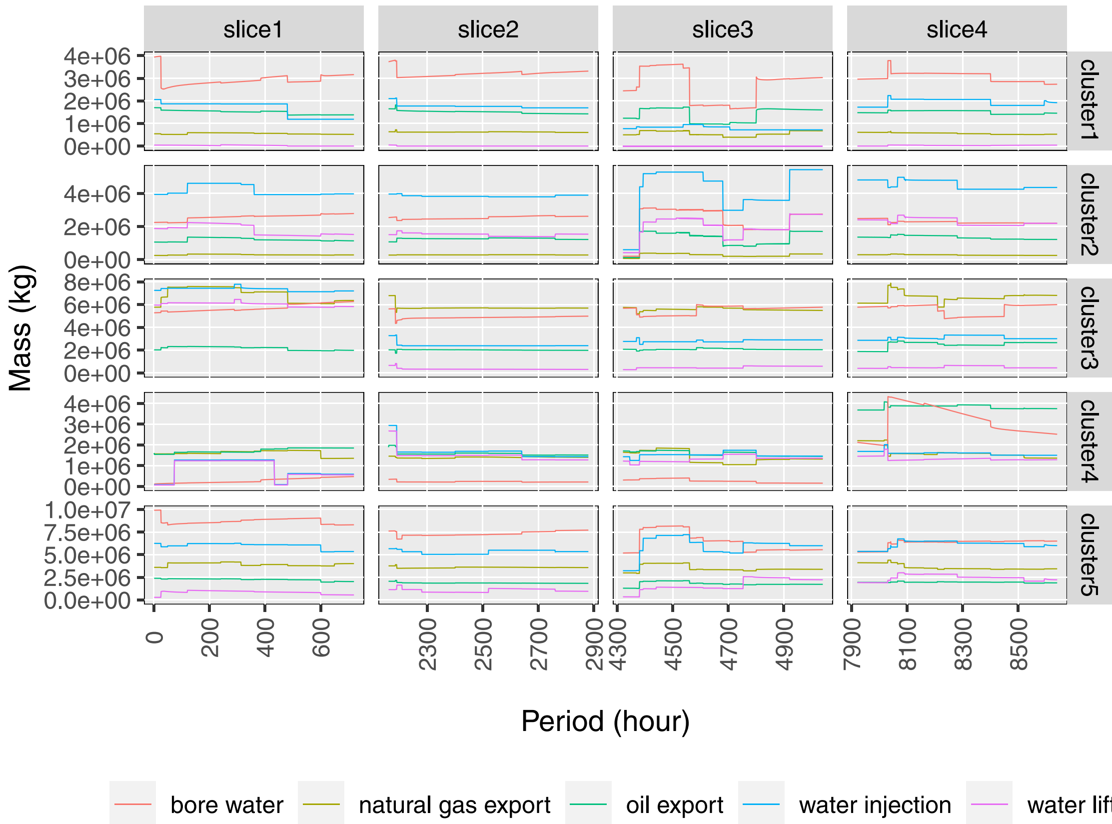

Fig. 7. Production profile in the representative months.

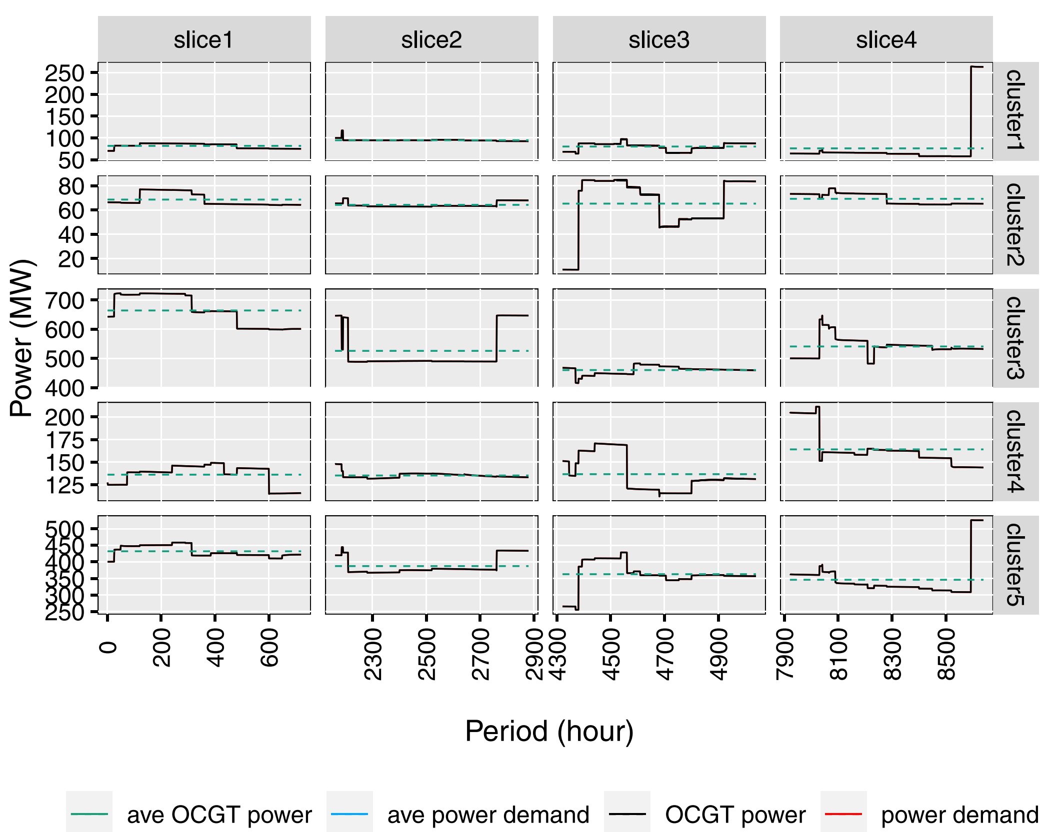

Fig. 8. Power consumption and supply (Only two lines are observable since power supply and demand match exactly. OCGT power equals power demand at all times).

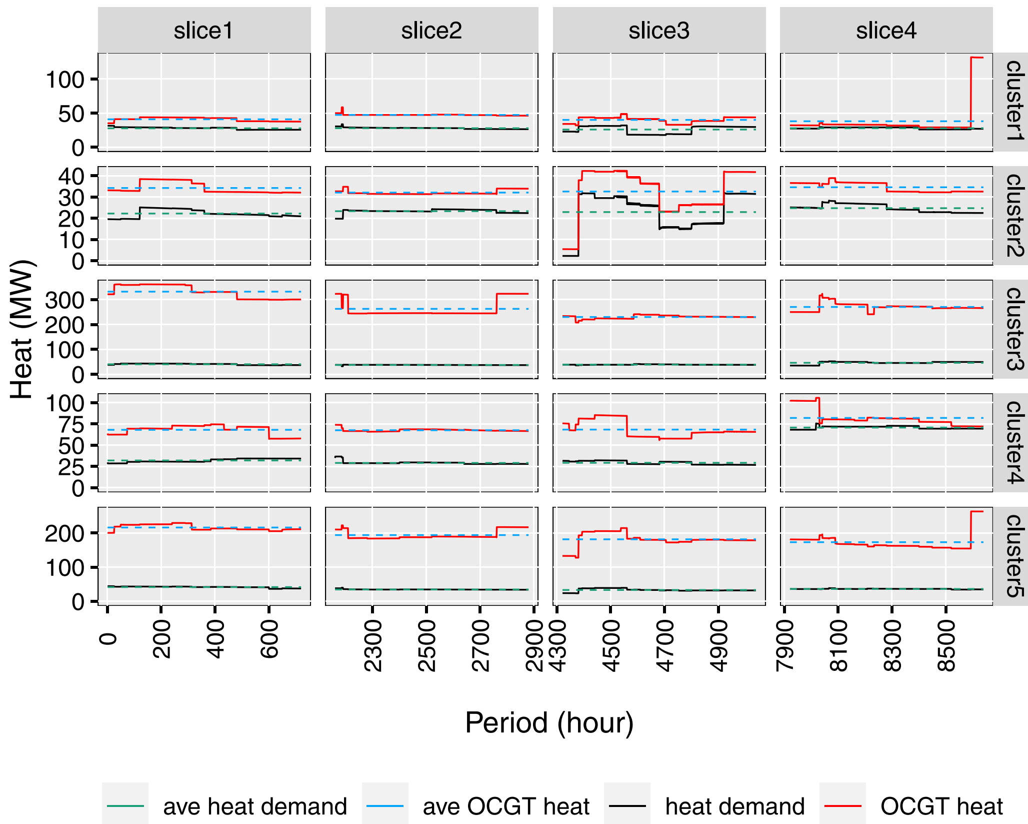

Fig. 9. Heat consumption and supply.

Fig. 10. Power demand in a year.

Table 1
Emission distribution by cluster.

	cluster1	cluster2	cluster3	cluster4	cluster5
Emission distribution	6.8%	5.5%	44.8%	11.7%	31.2%

in this study make up about 80% of the total load. Therefore, 5.54 Mt yearly emission is within the correct range, implying that the energy load modelling is relatively accurate.

From Fig. 8, we can see that the power output of the Open Cycle Gas Turbine (OCGT) matches the power demand at every operational period. Heat recovery of OCGTs is assumed to be the only heat source. Fig. 9 shows that heat recovery of OCGTs provides more than enough heat due to high electricity generation. We can also see that energy consumption can vary significantly. A breakdown of electricity load is shown in Fig. 10, gas export compressors dominate the power consumption in clusters 3–5. Water injection is the largest power consumer in cluster 2 since there are some mature fields (e.g., Ekofisk) whose reservoir pressures are mainly maintained by water injection. OCGT is the only energy and emission source in the initial setup. Therefore, emission breakdown includes the emissions from the total energy consumption of each region. Cluster 1 has the second smallest share of the total energy consumption, with a considerable amount of power consumed by gas injection. The fields in cluster 1, such as Grane, have the third-highest gas injection level among the 66 fields. From Table 1, we find that emission mainly comes from the northern part of the North Sea.

6.2. Sensitivity analysis of CO_2 tax

This section presents the results of sensitivity analysis of CO_2 tax. We introduce CO_2 tax and still keep the carbon budget inactive. We increase the carbon tax from 55 to 500 €/tonne with a step size of 5 €/tonne. PFS capacity limits are estimated from [61,81]. Note that the cost of PFS may be underestimated since we only consider the costs of subsea cables, onshore and offshore converter stations and electricity bills. In reality, PFS projects may also involve investment in onshore transmission lines or onshore power system capacity expansion. We analyse the results from three metrics: cost, CO_2 emission and energy

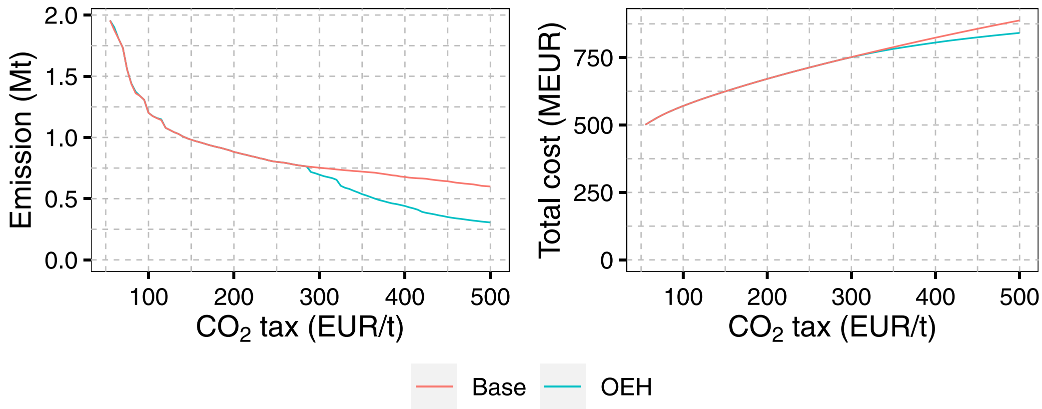

Fig. 11. Emission and cost comparison (CO_2 tax sensitivity analysis).

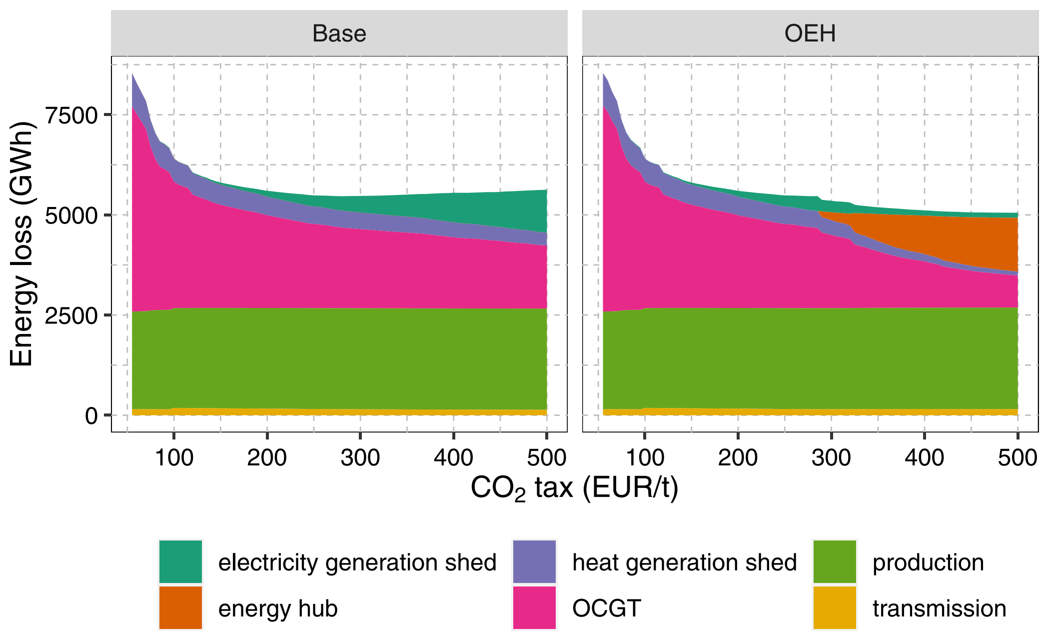

Fig. 12. Energy loss (CO_2 tax sensitivity analysis).

loss. Energy losses are from conversions, transmission, and generation shed. The calculation is presented in Appendix B.

From Fig. 11, we can see that CO_2 tax as a single instrument may not be enough to yield a zero emission system. We also find that near zero emission can be achieved with a very high CO_2 tax. Therefore, a hard carbon cap may be necessary for stimulating a zero emission system. When CO_2 tax is 55 €/tonne, the system reduces about 65% of the emissions compared to the initial 5.54 Mt/yr emission. Approximately 84% of the emissions can be cut if CO_2 tax is increased to 200 €/tonne as planned. As OCGTs are replaced by renewable energy, energy loss is reduced as well. OEHs can potentially reduce up to around 49% more CO_2 emission, and 5% total cost than the case with only offshore wind and PFS (Base) at certain CO_2 tax levels. From Fig. 12, we find that energy loss during production accounts for 11% of the energy loss. OCGTs lose 18 GWh of energy during an operational year. As production from wind turbines replaces gas turbines, energy loss from OCGT is reduced. However, due to the lack of energy storage, electricity generation shedding increases because wind power is shed. We find that OEHs can effectively reduce electricity generation shedding, although it loses energy during conversion. Overall, energy loss is up to 10% lower in the case of OEHs compared with Base at certain tax levels.

From Fig. 13, we find that different clusters show different levels of sensitivity to CO_2 tax. Offshore wind is the first renewable energy solution that is added to the system. Electric boilers are needed as offshore wind replaces gas turbines partially. OEHs are installed when CO_2 tax is above 290 €/tonne. Offshore solar is only added in cluster 5 under very high CO_2 tax levels. OCGTs still operate even CO_2 tax increases to 500 €/tonne. We can see that in a static planning problem, if CO_2 tax is the only instrument and increases to 200 €/tonne as the government's plan in 2030, OEHs may not be necessary. However, CO_2 tax combined with the EU emissions trading system may likely increase the total CO_2 price to around 250 – 300 €/tonne, which is about the breakeven price of OEHs. In addition, the potential benefits of the OEHs may realise once they provide services to more sectors, such as exporting hydrogen for industries or transportation.

6.3. Sensitivity analysis of CO_2 budget

For the CO_2 budget, we use initial emissions as the starting point, and reduce it by 5% until it hits 0. From Fig. 14, we find that the carbon cap is binding most of the time, and we rarely see that emissions are reduced more than the carbon cap. Thus, there is no difference in actual emissions in Base and the system with OEHs. However, the cost is 25% lower in a zero emission system with OEHs compared with Base.

We find that in a zero emission system without OEHs, energy loss is around 530 TWh due to 90 GW of wind power capacity and 15

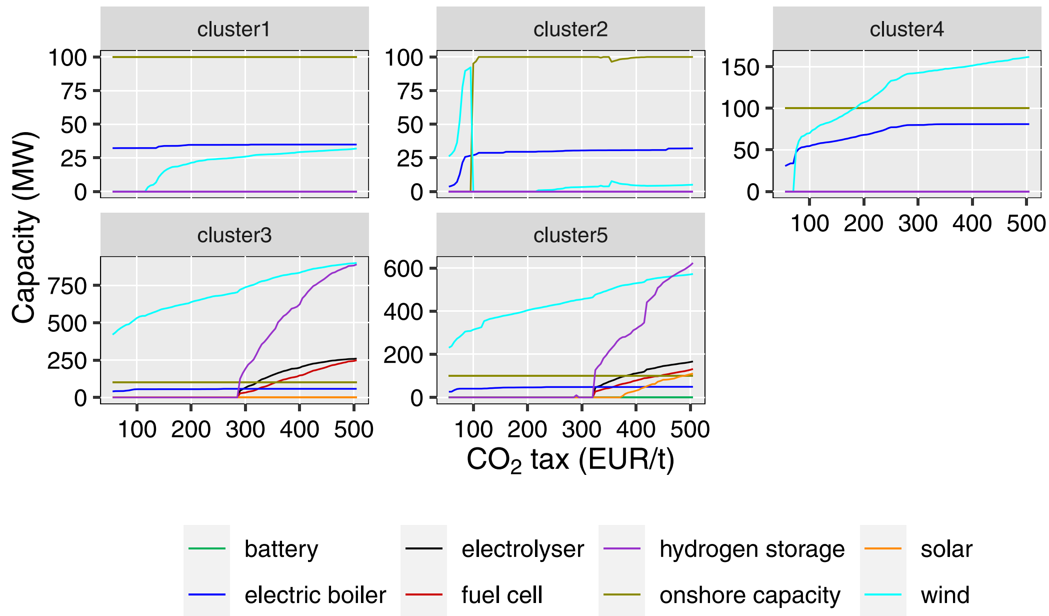

Fig. 13. Capacities of technologies in each cluster (CO_2 tax sensitivity analysis), hydrogen storage is measured in tonne.

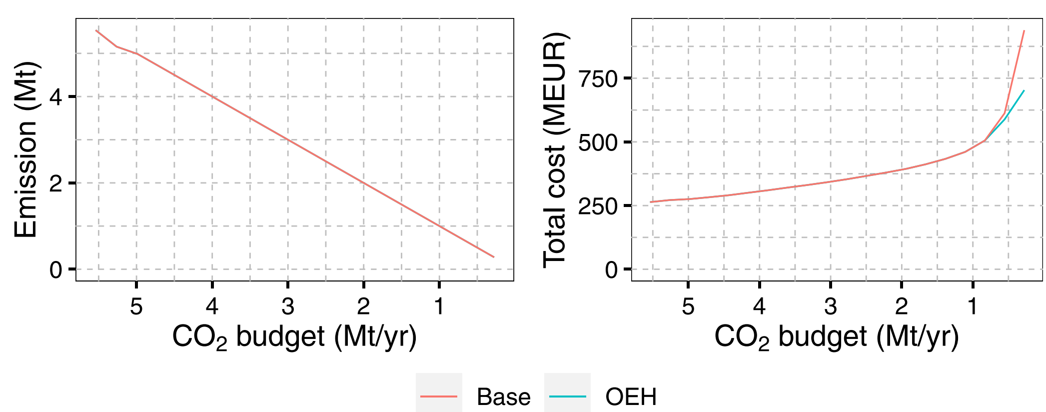

Fig. 14. Emission and cost comparison (CO_2 budget sensitivity analysis).

GW offshore solar capacity without storage. This may not be likely to happen since some forms of storage would be added to compensate for offshore wind in reality. From Fig. 15, we can see a large amount of energy loss when reaching near zero emission system in Base. The energy loss in Base is 10,749 GWh in a near zero emission system, which is about twice as high as for the case with OEHs. A large amount of wind power is installed to meet power demand at any time. Therefore, the same capacity of wind that can cope with peak demand hours, will also generate surplus power during normal hours. This leads to increased energy losses as more wind replaces OCGT without proper energy storage. In the case of OEHs, wind power can be stored when excess power is generated. It is also worth noticing that in the energy system without an OEH, energy storage is the battery on the platforms, which can be infeasible due to space and weight limitations. We observe that investments in batteries are only needed when approaching zero emission in Base. No battery is needed in a system with OEHs. In addition, the energy loss of OEHs is 28% of the total loss, and the loss during production is about 50% of the total.

From Fig. 16, we find that cluster 3 receives PFS after a 5% reduction of the carbon cap. Cluster 3 has the highest emission level but the shortest distance from shore. Therefore, taking PFS and partially electrifying the fields in cluster 3, can help the system reduce 5% of the emissions in a cost efficient way. The system does not cut emissions proportionally in each cluster, but cuts emissions from clusters with the highest emission, such as cluster 3 and cluster 5. Therefore, it may be necessary to consider the whole NCS when conducting system planning, rather than consider each cluster separately and reach sub-optimality. Cluster 2 is the most remote, more than 300 km from shore; PFS is less economical than offshore wind. Therefore, offshore wind is added to cluster 2 when the carbon cap drops to 2.77 Mt/yr. When the CO_2 budget reduces to below 0.83 Mt/yr, CO_2 emissions are nearly zero in clusters 1 and 2. However, the carbon cap needs to reduce to zero to shut down OCGTs completely in all clusters. Nearly 4,295 tonnes of hydrogen storage capacity is needed in a zero emission NCS energy system, and nearly half is installed in cluster 3.

6.4. Sensitivity analysis of the capacity of PFS

We now present the results of sensitivity analysis of the capacity of PFS. The capacity of PFS affects the investments in offshore technologies. An onshore system has a limited capacity to transmit power offshore. Although, onshore system expansion can affect this capacity limit, it is not considered directly in this paper. Therefore, we conduct sensitivity analysis to reveal the relationship between onshore power system capacity and offshore decarbonisation technologies.

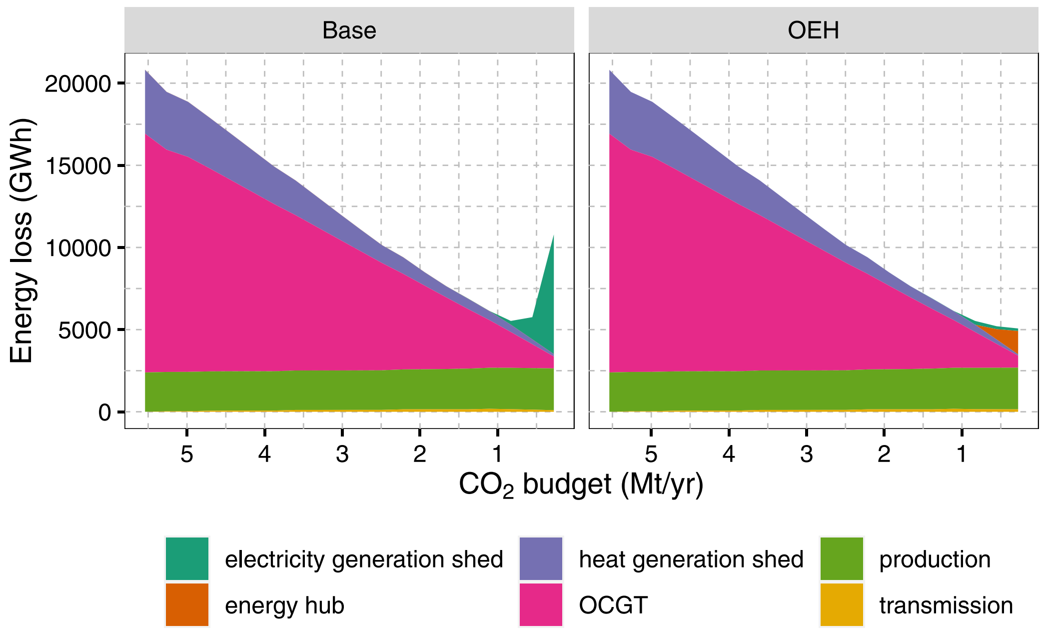

Fig. 15. Energy loss.(CO_2 budget sensitivity analysis)

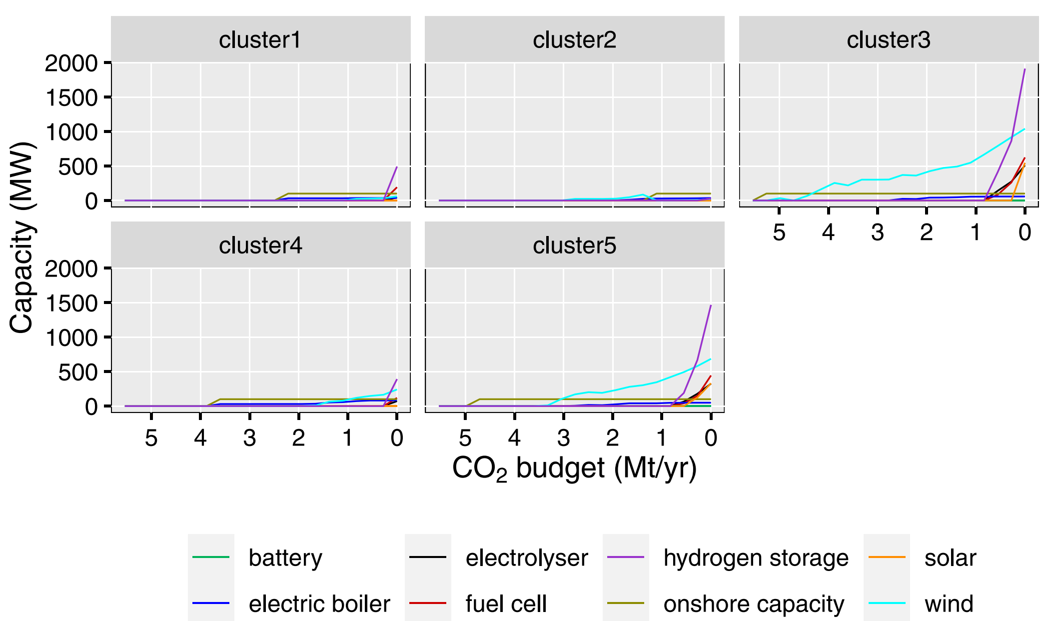

Fig. 16. Capacities of technologies in each cluster (CO_2 budget sensitivity analysis), hydrogen storage is measured in tonne.

6.4.1. Scenario 1 (S1)

The first scenario is to fix the CO_2 tax to 300 €/tonne, and increase the PFS capacity of each onshore location from 0 MW to 1,000 MW with a 10 MW step. The investment decisions remain the same when the PFS capacity is higher than 710 MW. Therefore, we only present the results from 0 MW to 710 MW. From Fig. 17, we can see that by having 710 MW capacity in each onshore location, the system can achieve 0.01 Mt/yr emission and reduce about 53% of the total cost. However, increasing the capacity further does not cut emissions or costs further. Fig. 19 shows that energy loss during transmission makes up 16% of the total energy loss as we increase the onshore capacity. Electricity generation shed decreases as onshore capacity increases because PFS gradually replaces offshore wind, and less energy is lost from wind turbines. From Fig. 18, we find that for onshore locations that connect to cluster 1 and cluster 2, the needed onshore capacities are about 126 MW and 108 MW, respectively. There are also upper limits on the installed capacity of PFS in the other clusters. We also notice that OEHs are still needed in clusters 3 and 5 as we increase the onshore capacity. However, eventually, OEHs are not needed since PFS can provide more stable power and OEH with storage becomes less important.

6.4.2. Scenario 2 (S2)

In the second scenario, the CO_2 tax is fixed to 400 €/tonne. We increase the onshore capacity from 0 MW to 1,000 MW, and present the results until 770 MW. From 20, we can see that without PFS, the system can achieve 0.63 Mt/yr emissions under S2 condition. Increasing the

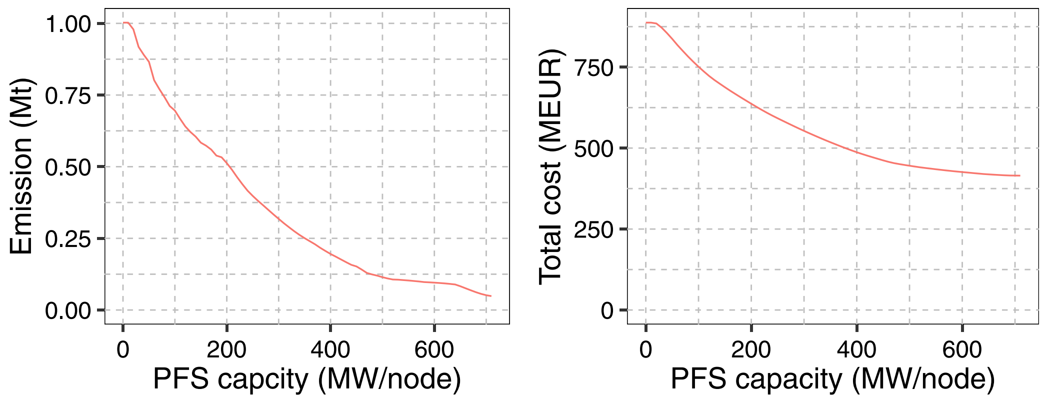

Fig. 17. Emission and cost (PFS capacity sensitivity analysis, S1).

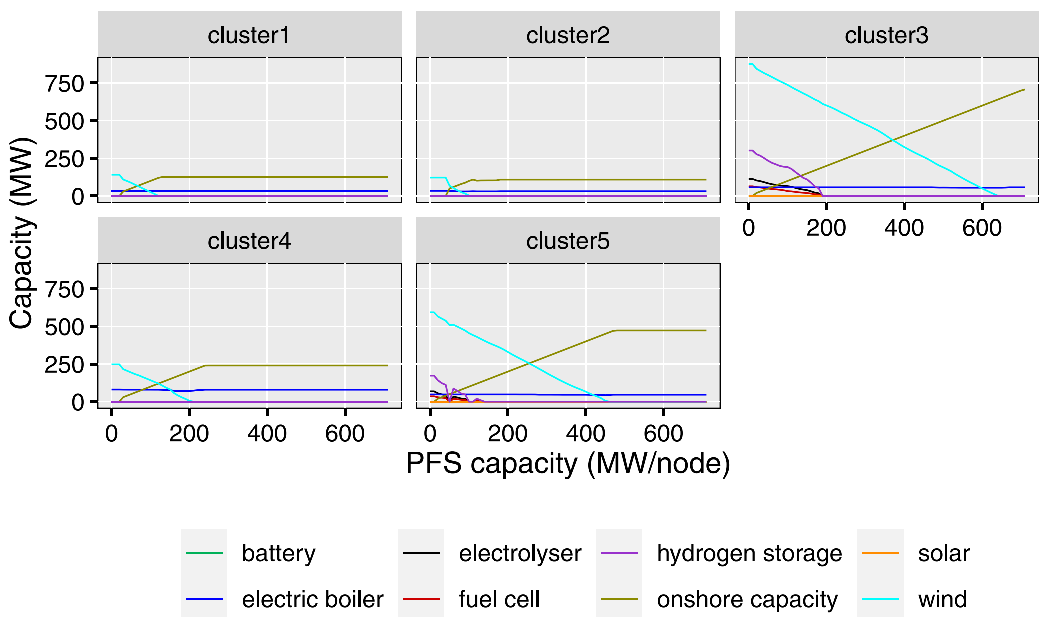

Fig. 18. Capacities of technologies in each cluster (PFS capacity sensitivity analysis, S1), hydrogen storage is measured in tonne.

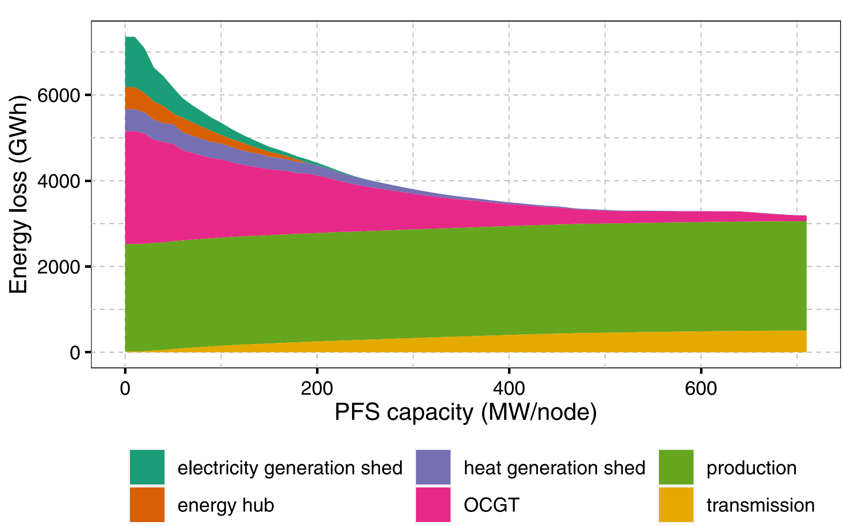

Fig. 19. Energy loss (PFS capacity sensitivity analysis, S1).

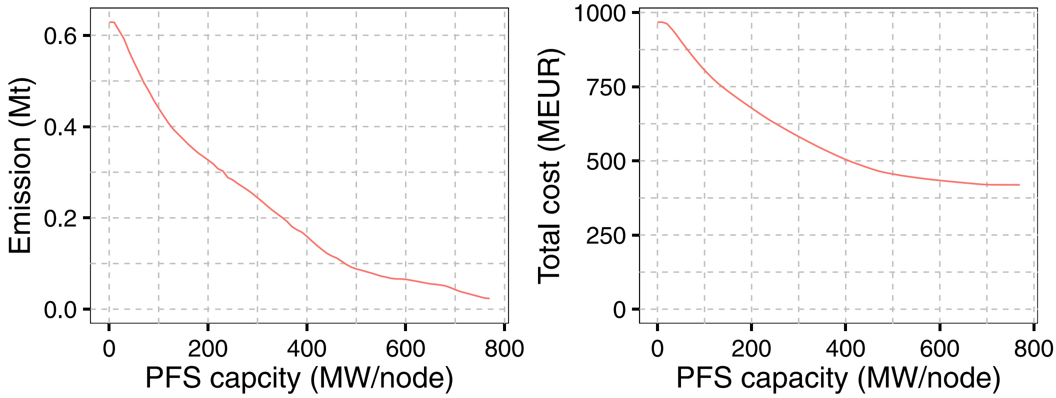

Fig. 20. Emission and cost (PFS capacity sensitivity analysis, S2).

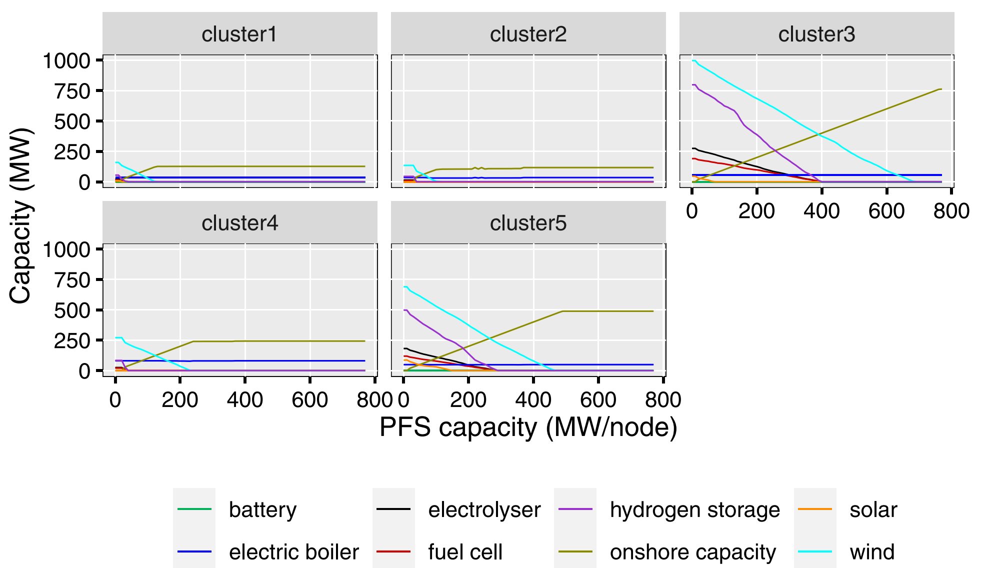

Fig. 21. Capacities of technologies in each cluster (PFS capacity sensitivity analysis, S2), hydrogen storage is measured in tonne.

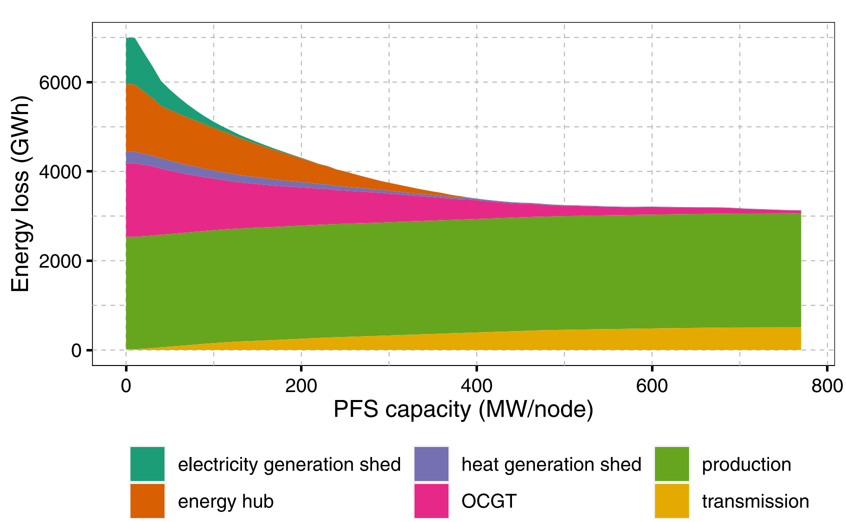

Fig. 22. Energy loss (PFS capacity sensitivity analysis, S2).

onshore capacity brings down 57% of the cost and also cut emission further to near zero. Fig. 22 shows that about 22% of the energy loss is from OEHs initially. OEHs are not needed when the onshore capacity increases to around 390 MW for each location. By adding the installed PFS capacity shown in Fig. 21, we find that a total onshore capacity of 1.74 GW may help the offshore energy system achieve near zero emission. We notice that the onshore system needs to provide an averagely of 1.4 GW. By checking the average power transmission of PFS, which might not be feasible without onshore system expansion.

7. Discussion

The analysis above shows that OEHs have potential value in emission reduction, energy losses and costs. The operational part of the model provides energy consumption of fields that is consistent with the analysis in [80], and aligned with officially reported numbers [59]. However, a similar investment planning problem is not found in the literature. Therefore, the results from the paper may provide a possible benchmark for future studies.

We demonstrate the case study on the NCS energy system. A unique characteristic of the NCS is that PFS is nearly emission free because nearly all Norwegian onshore power production is based on hydro power. However, in many regions, there may be less intention to use PFS because of the carbon intensity of the onshore power. In such a case, using PFS to compensate for offshore wind volatility may be infeasible, and hydrogen production and storage may become more relevant. This may affect the optimal investment planning of the system.

Based on the optimal solutions under different conditions showed in Figs. 13, 16, 18 and 21, we notice that offshore wind is a relatively cost efficient technology that can achieve moderate emission targets of platforms. This may suggest that in countries where PFS is not an option, offshore wind alone can still help emission reduction to a large extent.

In addition, the results suggest that producing and storing hydrogen offshore in OEHs proves to be economical under a strict carbon budget and a high CO_2 tax. One reason is that PFS is considered as an option for decarbonisation, and building cables is most likely cheaper than building an OEH. However, taking PFS will increase the pressure on the onshore system, and affect the security of supply of the onshore system and the onshore electricity price. This may cause public opposition. The potential restriction and limitation of the onshore power system may motivate offshore wind. Because OEHs can supply offshore platforms, a major function may be to supply and benefit the onshore system. Onshore wind power development is slow or even opposed in some regions. OEHs may help the onshore system decarbonisation by distributing offshore wind power to shore. Another insight is that a future hydrogen market may be needed in such a model to analyse the value of OEHs properly. Because the main function of OEHs is to supply offshore fields in the short- to mid-term, and serve for clean energy export in the long term. Including a hydrogen market can realise the long-term value of OEHs. The model can then be used for the techno-economical analysis of OEHs in onshore and offshore energy systems for countries with different energy policies in terms of offshore wind, onshore wind and green hydrogen.

Energy storage becomes very important in a system with higher wind power penetration. Hydrogen can be a promising option for long-term large-scale clean energy storage. Some offshore regions may have massive underground storage capacity. In such a case, the model can analyse whether OEHs with storage can be a cost-efficient solution for large-scale storage to help introduce more wind power in the system, and then help the energy transition towards zero emission.

Offshore energy system planning is of interest in many regions around the world. Decarbonising platforms may be a target during the planning in regions like the Gulf of Mexico and the Brazilian continental shelf. The model can be applied for the analysis of such locations. The model can also be used to analyse the interaction of an offshore energy system and onshore energy system transition. Regardless of the case study location, investment planning of an energy system typically aims to find optimal investment decisions that can fulfil the required energy load under some constraints. The model formulation is general, and there are no case-specific constraints. All locations and transmission lines are represented by nodes and arcs, respectively. A different configuration for each location and a cost model for each branch can be defined based on data. Model parameters, constraints, and variables can be modified according to the specific problem of the study.

Although the paper gives several insights and implications, the case study has some limitations: (a) we consider a simple network topology without considering the interconnections between fields clusters, and the interconnections may help OEHs distribute power; (b) we do not consider the capacity expansion of the onshore power system; and (c) we only consider using OEHs to decarbonise offshore fields, whereas, in reality, such hubs can provide service to more onshore and offshore industries, therefore, analysing OEHs also has relevance to onshore systems.

8. Conclusions and future work

This paper presents a multi-carrier offshore energy system investment planning optimisation model with a high degree of operational detail to find cost-optimal solutions for decarbonising NCS energy supply. The major novelties and contributions are: (1) formulating OEHs in an integrated MILP investment and operational model for large-scale offshore energy system planning; (2) modelling the device-level energy consumption of the offshore platforms with hourly time resolution on a large scale; and (3) conducting a large-scale analysis of the value of OEHs in the North Sea offshore energy system transition towards decarbonised energy supply. Results from our case study indicate that: (1) OEHs can reduce up to 10% of the energy loss and 49% of the emissions with CO_2 tax above 290 €/tonne; (2) OEHs can reduce energy loss by 53% in a near zero emission system; (3) a carbon budget may be necessary to enable a zero emission energy system in addition to CO_2 tax; and (4) the system cuts about 65% of the initial emissions when CO_2 tax is 55 €/tonne, and approximately 84% of the CO_2 emissions can be cut if CO_2 tax is increased to Norway's target of 200 €/tonne.

Although the deterministic MILP model in this paper has led to many insights, there are several possible extensions. A deterministic optimisation model is not capable of representing load and supply uncertainties. Therefore, we aim to develop a stochastic optimisation model [82] and incorporate long-term and short-term uncertainties in future work. In addition, multiple investment stages are needed to represent the investment planning problem more realistically. Besides, we only consider using OEHs for fields decarbonisation, which makes OEHs seem less attractive than other technologies due to their high costs. However, OEHs can have various advantages such as energy provision to offshore fish farming, maritime transport, and using the infrastructure past the lifetime of the oil and gas fields for purposes such as exporting hydrogen. These may motivate the investments in OEHs, which we aim to include some of the aspects in future. Finally, more work can be done on offshore network topology and the representation of the onshore power system.

CRediT authorship contribution statement

Hongyu Zhang: Conceptualization, Methodology, Software, Validation, Formal analysis, Investigation, Visualisation, Data curation, Writing – original draft, Writing – review & editing. **Asgeir Tomasgard:** Conceptualization, Supervision, Writing – review & editing, Funding acquisition. **Brage Rugstad Knudsen:** Conceptualization, Supervision, Writing – review & editing. **Harald G. Svendsen:** Conceptualization, Writing – review & editing. **Steffen J. Bakker:** Conceptualization, Writing – review & editing. **Ignacio E. Grossmann:** Conceptualization, Supervision, Writing – review & editing.

Declaration of competing interest

The authors declare that they have no known competing financial interests or personal relationships that could have appeared to influence the work reported in this paper.

Data availability

We have shared the link to all the data and code.

Acknowledgements

This work was supported by the Research Council of Norway through PETROSENTER LowEmission (project code 296207). We appreciate the input from Per Eirik Bergmo, Heiner Schümann and Torleif Holt, SINTEF Industry, Magnus Korpås, Department of Electric Power Engineering, NTNU and Espen Flo Bødal, SINTEF Energy Research.

Appendix A. Nomenclature

Investment planning related sets

$\mathcal{I}$	set of operational nodes
$\mathcal{I}_0$	set of investment nodes
$\mathcal{I}_i$	set of investment nodes i ($i \in \mathcal{I}_0$) ancestor to operational node i ($i \in \mathcal{I}$)
$\mathcal{P}$	set of technologies

Operation related sets

$\mathcal{B}^E$	set of electric boilers
$\mathcal{C}$	set of compressors
$\mathcal{E}$	set of electrolysers
$\mathcal{F}$	set of fuel cells
$\mathcal{G}$	set of gas turbines
$\mathcal{L}$	set of subsea cables
$\mathcal{N}$	set of time slices
$\mathcal{P}^*$	set of all electric boilers, electrolysers and fuel cells ($\mathcal{P}^* = \mathcal{B}^E \cup \mathcal{E} \cup \mathcal{F}$)
$\mathcal{P}^U$	set of pumps
$\mathcal{R}$	set of renewable units (offshore wind and offshore solar)
$\mathcal{S}^E$	set of electricity storage
$\mathcal{S}^{Hy}$	set of hydrogen storage facilities
$\mathcal{T}$	set of hours in all time slices
$\mathcal{T}_n$	set of hours in time slice n ($n \in \mathcal{N}$)
$\mathcal{Z}$	set of all locations, including platforms $\mathcal{Z}^P$, OEHs $\mathcal{Z}^H$, and onshore buses $\mathcal{Z}^O$ ($\mathcal{Z} = \mathcal{Z}^P \cup \mathcal{Z}^H \cup \mathcal{Z}^O$)

Investment planning related parameters

κ	scaling effect depending on time step between successive investment nodes
C_{pi}^{Fix}	unitary fix operational and maintenance cost of technology p in operational node i ($p \in \mathcal{P}, i \in \mathcal{I}$) [€/MW, €/MWh, €/kg]
C_{pi}^{InvF}	fixed capacity independent investment cost of technology p in investment node i ($p \in \mathcal{P}, i \in \mathcal{I}_0$) [€]
C_{pi}^{InvV}	unitary investment cost of technology p in investment node i ($p \in \mathcal{P}, i \in \mathcal{I}_0$) [€/MW, €/MWh, €/kg]
Q_p	capacity of a unit of technology p ($p \in \mathcal{P}$) [MW, MWh, kg]
X_p^{Max}	maximum accumulated capacity of technology p ($p \in \mathcal{P}$) [MW, MWh, kg]
Y_{pi}	maximum number of newly invested units of technology p in investment node i ($p \in \mathcal{P}, i \in \mathcal{I}_0$)

Operation related parameters

α_g^G/α_f^F	maximum ramp rate of gas turbines /fuel cells ($g \in \mathcal{G}, f \in \mathcal{F}$) [MW/MW]
η^*	efficiency of compressors, electric boilers, fuel cells, gas turbines, heat recovery of gas turbines electric storage and transmission lines $* = \{$C, BE, F, G, HrG, SE, L$\}$ indexed by related sets
η^{EF}	conversion factor of electrolyser to inject hydrogen directly to fuel cell [MWh/kg]
η^{ES}	conversion factor of electrolyser to inject hydrogen to the storage facility [MWh/kg]
γ_s^{SE}	power ratio of electricity store s ($s \in \mathcal{S}^E$) [MW/MWh]
μ^E	yearly CO_2 emission limit (tonne)
ρ_f^F	hydrogen consumption factor of fuel cell f ($f \in \mathcal{F}$) [kg/MW]
σ_z^{Res}	spinning reserve factor on platform z ($z \in \mathcal{Z}^P$)
τ_{zt}^{EP}	electricity price in onshore bus z in period t ($z \in \mathcal{Z}^O, t \in \mathcal{T}$) [€/MW]
C_g^G	total operational cost of gas turbine g ($g \in \mathcal{G}$) [€/MW]
$C^{Shed,l}$	load shed penalty cost of power ($l = P$) and heat ($l = H$) [€/MW]
C_g^G	total operational cost of generating 1 MW power from gas turbine g ($g \in \mathcal{G}$) [€/MW]
E_g^G	emission factor of gas turbine g ($g \in \mathcal{G}$) [tonne/MWh]
E_g^G	emission of CO_2 of gas turbine g burning fuel ($g \in \mathcal{G}$) [t/MWh]
H_t	number of hour(s) in one operational period t
P_{zt}^{DP}	power demand on platform z period t ($z \in \mathcal{Z}, t \in \mathcal{T}$) [MW]
R_{rt}^R	capacity factor of renewable unit r in period t ($r \in \mathcal{R}, t \in \mathcal{T}$)
W_t	weighted length of one operational period t

Investment planning related variables

c^{INV}	total investment and fixed operating and maintenance costs [€]
c_i^{OPE}	total operational costs in operational node i ($i \in \mathcal{I}$)[€]
x_{pi}^{Acc}	accumulated capacity of device p in operational node i ($p \in \mathcal{P}, i \in \mathcal{I}$) [MW, MWh, kg]
x_{pi}^{Inst}	newly invested capacity of device p in investment node i_0 ($p \in \mathcal{P}, i \in \mathcal{I}_0$) [MW, MWh, kg]
y_{pi}	number of units of newly invested technology p in investment node i_0 ($p \in \mathcal{P}, i \in \mathcal{I}_0$)

Operation related variables

p_{et}^E	power consumption of electrolyser e in period t ($e \in \mathcal{E}, t \in \mathcal{T}$) [MW]
p_{ft}^F	power generation of fuel cell f in period t ($f \in \mathcal{F}, t \in \mathcal{T}$) [MW]
p_{bt}^{BE}	power consumption of electric boiler b in period t ($b \in \mathcal{B}^E, t \in \mathcal{T}$) [MW]
p_f^{AccF}	accumulated capacity of fuel cell f ($f \in \mathcal{F}, t \in \mathcal{T}$) [MW]
p_{gt}^G	power generation of gas turbine g in period t ($g \in \mathcal{G}, t \in \mathcal{T}$) [MW]
p_{gt}^{ResG}	power reserved of gas turbine g for spinning reserve requirement in period t ($g \in \mathcal{G}, t \in \mathcal{T}$) [MW]
p_g^{AccG}	accumulated capacity of gas turbine g ($g \in \mathcal{G}$) [MW]
p_{lt}^L	power flow in line l in period t ($l \in \mathcal{L}, t \in \mathcal{T}$) [MW]
p_l^{AccL}	accumulated capacity of line l ($l \in \mathcal{L}$) [MW]
p_{st}^{ResSE}	power reserved in electricity store s for spinning reserve requirement in period t ($s \in \mathcal{S}^E, t \in \mathcal{T}$) [MW]
$p_{st}^{SE+}/p_{st}^{SE-}$	charge/discharge power of electricity store s in period t ($s \in \mathcal{S}^E, t \in \mathcal{T}$) [MW]
$p_{zt}^{GShed,l}$	generation shed for power ($l = P$) and heat ($l = H$) at z in period t ($z \in \mathcal{Z}, t \in \mathcal{T}$) [MW]

Table D.2
Field location data.

Field	Longtitude	Latitude	Cluster	Distance to centre (km)	Field	Longtitude	Latitude	Cluster	Distance to centre (km)
ALVHEIM	1.94	59.54	4	21.28	OSEBERG SØR	2.94	60.31	4	56.09
ATLA	2.57	59.65	4	26.79	REV	1.92	58.02	4	55.10
BØYLA	1.89	59.29	4	28.83	RINGHORNE ØST	2.51	59.27	4	24.71
BALDER	2.41	59.27	4	22.46	SIGYN	2.02	58.28	4	27.28
BLANE	2.49	56.84	2	51.14	SINDRE	2.35	61.23	2	8.90
BRAGE	3.06	60.48	1	36.29	SKIRNE	2.47	59.60	1	18.79
BYRDING	3.53	61.13	1	41.11	SKOGUL	2.22	59.78	1	35.63
EDVARD GRIEG	2.33	58.85	3	43.47	SLEIPNER ØST	1.98	58.41	3	12.61
EKOFISK	3.23	56.49	2	10.82	SLEIPNER VEST	1.66	58.39	2	20.45
ELDFISK	3.32	56.38	2	24.70	SNORRE	2.06	61.40	2	17.81
EMBLA	3.27	56.29	2	33.02	STATFJORD	1.80	61.17	2	22.36
ENOCH	1.52	58.63	3	26.41	STATFJORD ØST	1.99	61.31	3	12.38
FLYNDRE	2.63	56.55	2	34.31	STATFJORD NORD	1.91	61.43	2	24.38
FRAM	3.48	61.05	1	31.54	SVALIN	2.40	59.14	1	36.57
FRAM H-NORD	3.50	61.10	1	37.58	SYGNA	2.00	61.46	1	25.91
GIMLE	2.35	61.25	5	8.59	TAMBAR	3.01	56.94	5	40.88
GINA KROG	1.70	58.54	3	12.92	TOR	3.30	56.63	3	8.07
GJØA	3.93	61.30	1	68.12	TORDIS	2.11	61.25	1	3.81
GRANE	2.44	59.11	4	39.71	TROLL	3.91	60.50	4	48.72
GUDRUN	1.72	58.81	3	34.85	TRYM	4.24	56.40	3	67.95
GULLFAKS	2.12	61.19	5	7.32	TUNE	2.61	60.41	5	54.21
GULLFAKS SØR	2.03	61.17	5	12.55	ULA	2.87	57.07	5	56.73
GUNGNE	1.89	58.35	3	18.34	UTGARD	1.54	58.34	3	29.08
HEIMDAL	2.22	59.55	4	10.21	VALE	2.29	59.68	4	24.91
HOD	3.43	56.18	2	48.13	VALEMON	2.25	60.99	2	28.90
ISLAY	1.93	60.54	5	79.72	VALHALL	3.43	56.23	5	42.42
IVAR AASEN	2.12	58.92	3	46.13	VEGA	3.36	61.34	3	61.26
JOHAN SVERDRUP	2.63	58.66	3	43.96	VESLEFRIKK	2.88	60.74	3	20.24
KNARR	2.71	61.78	5	65.69	VIGDIS	2.12	61.34	5	10.65
KVITEBJØRN	2.48	61.04	5	27.90	VILJE	2.28	59.64	5	20.43
ODA	3.04	57.06	2	53.15	VISUND	2.62	61.42	2	29.58
OSEBERG	2.69	60.54	1	40.92	VISUND SØR	2.34	61.27	1	8.44
OSEBERG ØST	2.96	60.58	1	27.71	VOLUND	2.00	59.45	1	15.66

p^{PFS}_{zt} power supply from onshore bus z in period t ($z \in \mathcal{Z}^O, t \in \mathcal{T}$) [MW]
$p^{Shed,l}_{zt}$ load shed for power ($l = P$) and heat ($l = H$) at z in period t ($z \in \mathcal{Z}, t \in \mathcal{T}$) [MW]
q^{SE}_{st} energy level of electricity store s at the start of period t ($s \in \mathcal{S}^E, t \in \mathcal{T}$) [MWh]
q^{AccSE}_{s} accumulated storage capacity of electricity store s ($s \in \mathcal{S}^E$) [MWh]
$v^{SHy+}_{st}/v^{SHy-}_{st}$ injection/withdraw of hydrogen to (from) hydrogen storage s in period t ($s \in \mathcal{S}^{Hy}, t \in \mathcal{T}$) [kg]
v^{SHy}_{st} storage level of hydrogen storage s in period t ($s \in \mathcal{S}^{Hy}, z \in \mathcal{Z}^H, t \in \mathcal{T}$) [kg]
v^{AccSHy}_{s} accumulated storage capacity of hydrogen store s ($s \in \mathcal{S}^{Hy}, t \in \mathcal{T}$) [kg]

Appendix B. Calculation of energy loss

The indices, summation and multiplication of one hour are omitted.

$$q^{Loss} = p^{GShed} + p^{GShedH} + (\frac{1}{\eta^G} - 1 - \eta^{HrG})p^G + (1-\eta^l)p^l + p^E - \theta^{Hy}(\frac{p^F}{\eta^F\theta^{Hy}} - v^{SHy-} + v^{SHy+}) + (\frac{1}{\eta^F} - 1)p^F,$$

where $(1-\eta^l)p^l$ calculates the total energy losses of electricity storage, separators, compressors, pumps, electric boilers and transmission lines. The hydrogen energy content is denoted by θ^{Hy}.

Appendix C. Definitions of model parameters

The total operational cost of a gas turbine is defined by

$$C^G_g = C^{OPEX}_g + \frac{C^{Fuel}_g + C^{CO_2}E^{Fuel}_g}{\eta^G_g}, \tag{C.1}$$

and the emission factor of gas turbine is defined by

$$E^G_g = \frac{E^{Fuel}_g}{\eta^G_g}, \tag{C.2}$$

where C^{OPEX}_g is the variable operational cost of gas turbines. The E^{Fuel}_g is the fuel cost of gas turbines burning fuel with energy content 1 MWh. The parameter E^{Fuel}_g is the emission of CO_2 of gas turbines burning fuel with energy content 1 MWh. The efficiency of gas turbines is denoted by η^G_g.

Power demand of a platform

$$P^{DP}_{zt} = \sum_{c\in C_z} \frac{V^C_{zt}ZRT}{\eta^C(\alpha-1)}\left(\gamma_c^{\frac{\alpha-1}{\alpha}} - 1\right) + \sum_{p\in\mathcal{P}^U_z} \kappa^{Pu}_p V^{Pu}_{pt}, \tag{C.3}$$

equals to the power consumption of all compressors and all pumps. The power consumption of a compressor is given by $\frac{V^C_{zt}ZRT}{\eta^C(\alpha-1)}\left(\gamma_c^{\frac{\alpha-1}{\alpha}} - 1\right)$, where V^C_{zt} is the gas compressed by a compressor, η^C is the isentropic efficiency of a compressor, α is the polytropic exponent of a compressor, γ_c is the compression ratio of a compressor, Z is compressibility factor, R is the characteristic gas constant and T is the temperature. The power consumption of a pump is given by $\kappa^{Pu}_p V^{Pu}_{pt}$, where V^{Pu}_{pt} is the fluid pumped by a pump, κ^{Pu}_p is the electricity demand as fraction of amount of fluid pumped. The detailed derivation of power consumption of compressors and pumps is presented in [83].

Hydrogen consumption factor of fuel cell is given by

$$\rho^F = \frac{1}{\eta^F_f \theta^{Hy}}, \tag{C.4}$$

where η^F_f is the efficiency of fuel cells and θ^{Hy} is the energy content of hydrogen.

Weighted length of a operational period is defined by

$$W_t = W^N_n H_t, \quad n \in \mathcal{N}, t \in \mathcal{T}^N, \tag{C.5}$$

where W^N_n is the weight of each slice n and H_t is the length of operational period t.

Appendix D. Input data

Table D.2 provides an overview over the locations of the different fields.

References

[1] IEA. Renewables 2020. 2020, URL: https://www.iea.org/reports/renewables-2020. [Accessed March 2022].

[2] European Commission. A European green deal. 2020, https://ec.europa.eu/info/strategy/priorities-2019-2024/european-green-deal_en. [Accessed June 2021].

[3] North Sea Wind Power Hub Programme. North Sea wind power hub. 2021, https://northseawindpowerhub.eu. [Accessed May 2021].

[4] Geidl M, Koeppel G, Favre-Perrod P, Klockl B, Andersson G, Frohlich K. Energy hubs for the future. IEEE Power Energy Mag 2007;5(1):24–30. http://dx.doi.org/10.1109/MPAE.2007.264850.

[5] European Commission. Boosting offshore renewable energy for a climate neutral Europe. 2020, https://ec.europa.eu/commission/presscorner/detail/en/IP_20_2096. [Accessed July 2021].

[6] Piacentino A, Duic N, Markovska N, Mathiesen BV, Guzović Z, Eveloy V, et al. Sustainable and cost-efficient energy supply and utilisation through innovative concepts and technologies at regional, urban and single-user scales. Energy 2019;182:254–68. http://dx.doi.org/10.1016/j.energy.2019.06.015.

[7] Østergaard PA, Duic N, Noorollahi Y, Kalogirou SA. Recent advances in renewable energy technology for the energy transition. Renew Energy 2021;179:877–84. http://dx.doi.org/10.1016/j.renene.2021.07.111.

[8] Vujanović M, Wang Q, Mohsen M, Duić N, Yan J. Recent progress in sustainable energy-efficient technologies and environmental impacts on energy systems. Appl Energy 2021;283:116280. http://dx.doi.org/10.1016/j.apenergy.2020.116280.

[9] Kovač A, Paranos M, Marciuš D. Hydrogen in energy transition: A review. Int J Hydrogen Energy 2021;46(16):10016–35. http://dx.doi.org/10.1016/j.ijhydene.2020.11.256.

[10] European Commission. REPowerEU: affordable, secure and sustainable energy for Europe. 2022, https://ec.europa.eu/info/strategy/priorities-2019-2024/european-green-deal/repowereu-affordable-secure-and-sustainable-energy-europe_en. [Accessed June 2022].

[11] Bosch J, Staffell I, Hawkes AD. Temporally explicit and spatially resolved global offshore wind energy potentials. Energy 2018;163:766–81. http://dx.doi.org/10.1016/j.energy.2018.08.153.

[12] Thommessen C, Otto M, Nigbur F, Roes J, Heinzel A. Techno-economic system analysis of an offshore energy hub with an outlook on electrofuel applications. Smart Energy 2021;3:100027. http://dx.doi.org/10.1016/j.segy.2021.100027.

[13] Singlitico A, Østergaard J, Chatzivasileiadis S. Onshore, offshore or in-turbine electrolysis? Techno-economic overview of alternative integration designs for green hydrogen production into Offshore Wind Power Hubs. Renew Sustain Energy Transit 2021;1:100005. http://dx.doi.org/10.1016/j.rset.2021.100005.

[14] Scafidi J, Wilkinson M, Gilfillan SM, Heinemann N, Haszeldine RS. A quantitative assessment of the hydrogen storage capacity of the UK continental shelf. Int J Hydrogen Energy 2021;46(12):8629–39. http://dx.doi.org/10.1016/j.ijhydene.2020.12.106.

[15] Dincer I, Cozzani V, Crivellari A. Hybrid Energy Systems for Offshore Applications. Hybrid Energy Systems, Elsevier; 2021, http://dx.doi.org/10.1016/C2020-0-02794-5.

[16] Zhang A, Zhang H, Qadrdan M, Li X, Li Q. Energy hub based electricity generation system design for an offshore platform considering CO2-mitigation. Energy Procedia 2017;142:3597–602. http://dx.doi.org/10.1016/j.egypro.2017.12.250.

[17] Mikkola E, Heinonen J, Kankainen M, Hekkala T, Kurkela J. Multi-platform concepts for combining offshore wind energy and fish farming in freezing sea areas: Case study in the Gulf of Bothnia. In: Proceedings of the International Conference on Offshore Mechanics and Arctic Engineering - OMAE. 6, 2018, http://dx.doi.org/10.1115/OMAE2018-77677.

[18] Elgenedy M, Ahmed K, Burt G, Rogerson G, Jones G. Unlocking the UK continental shelf electrification potential for offshore oil and gas installations: A power grid architecture perspective. Energies 2021;14(21). http://dx.doi.org/10.3390/en14217096.

[19] Bret-Rouzaut N, Favennec J, Babusiaux D, Pearse J. Oil and Gas Exploration and Production : Reserves, Costs, Contracts. Editions Technips; 2011, http://dx.doi.org/10.5860/choice.42-4042.

[20] Fazeres-Ferradosa T, Rosa-Santos P, Taveira-Pinto F, Vanem E, Carvalho H, Correia J. Advanced research on offshore structures and foundation design: Part 1. In: Proceedings of the Institution of Civil Engineers-Maritime Engineering. 172, 2019, p. 118–23. http://dx.doi.org/10.1680/jmaen.2019.172.4.118.

[21] Farrokhifar M, Nie Y, Pozo D. Energy systems planning: A survey on models for integrated power and natural gas networks coordination. Appl Energy 2020;262:114567. http://dx.doi.org/10.1016/j.apenergy.2020.114567.

[22] Böhringer C, Rutherford TF. Combining bottom-up and top-down. Energy Econ 2008;30(2):574–96. http://dx.doi.org/10.1016/j.eneco.2007.03.004.

[23] Backe S, Skar C, del Granado PC, Turgut O, Tomasgard A. EMPIRE: An open-source model based on multi-horizon programming for energy transition analyses. SoftwareX 2022;17:100877. http://dx.doi.org/10.1016/j.softx.2021.100877.

[24] Burandt T, Löffler K, Hainsch K. GENeSYS-MOD v2.0 - Enhancing the Global Energy System Model: Model improvements, framework changes, and European data set. (94). Deutsches Institut für Wirtschaftsforschung (DIW); 2018, URL: http://hdl.handle.net/10419/180395. [Accessed June 2022].

[25] Lara CL, Siirola JD, Grossmann IE. Electric power infrastructure planning under uncertainty: stochastic dual dynamic integer programming (SDDiP) and parallelization scheme. Opt Eng 2019;1–39. http://dx.doi.org/10.1007/s11081-019-09471-0.

[26] Gupta V, Grossmann IE. An efficient multiperiod MINLP model for optimal planning of offshore oil and gas field infrastructure. Ind Eng Chem Res 2012;51(19):6823–40. http://dx.doi.org/10.1021/ie202959w.

[27] Flórez-Orrego D, Albuquerque C, da Silva JA, Freire RLA, de Oliveira Junior S. Optimal design of power hubs for offshore petroleum platforms. Energy 2021;235:121353. http://dx.doi.org/10.1016/j.energy.2021.121353.

[28] Jansen M, Duffy C, Green TC, Staffell I. Island in the Sea: The prospects and impacts of an offshore wind power hub in the North Sea. Adv Appl Energy 2022;6:100090. http://dx.doi.org/10.1016/j.adapen.2022.100090.

[29] Gondal IA. Offshore renewable energy resources and their potential in a green hydrogen supply chain through power-to-gas. Sustain Energy Fuels 2019;3:1468–89. http://dx.doi.org/10.1039/C8SE00544C.

[30] Marchand J, Shetgaonkar A, Rueda Torres JL, Lekic A, Palensky P. EMT real-time simulation model of a 2 GW offshore renewable energy hub integrating electrolysers. Energies 2021;14(24). http://dx.doi.org/10.3390/en14248547.

[31] van der Veer E, Sweers B, Kawale D, van Unen M, van Schot M, Kee J, et al. North Sea energy offshore energy islands deliverable D3.8. North Sea Energy 2019. URL: https://north-sea-energy.eu/static/0856dd12a36d1f321aaf757706bd5913/8a.-FINAL-NSE3_D3.8-Final-report-on-the-techno-economic-environmental-and-legal-assessment-of-offshore-energy-islands.pdf. [Accessed June 2021].

[32] Tosatto A, Beseler XM, Østergaard J, Pinson P, Chatzivasileiadis S. North Sea Energy islands: Impact on national markets and grids. 2021, arXiv:10.48550/arXiv.2103.17056.

[33] Kitzing L, González MG. Market arrangements for offshore wind energy networks. Technical University of Denmark (DTU); 2020, URL: https://backend.orbit.dtu.dk/ws/portalfiles/portal/222047192/NSON_DK_WP5_offshore_market_arrangements_final.pdf. [Accessed June 2021].

[34] Armeni A, Semenyuk M, Plet C, Kitzing L, González M, Grønlund Arnklit A, et al. D12.5 deployment plan for future European offshore grid development. short-term project – Bornholm island CleanStream energy hub.. Technical University of Denmark (DTU); 2021, URL: https://orbit.dtu.dk/en/publications/d125-deployment-plan-for-future-european-offshore-grid-developmen. [Accessed June 2022].

[35] Ottesen SO, Tomasgard A. A stochastic model for scheduling energy flexibility in buildings. Energy 2015;88:364–76. http://dx.doi.org/10.1016/j.energy.2015.05.049.

[36] Ødegaard Ottesen S, Tomasgard A, Fleten S-E. Prosumer bidding and scheduling in electricity markets. Energy 2016;94:828–43. http://dx.doi.org/10.1016/j.energy.2015.11.047.

[37] Ayele GT, Haurant P, Laumert B, Lacarrière B. An extended energy hub approach for load flow analysis of highly coupled district energy networks: Illustration with electricity and heating. Appl Energy 2018;212:850–67. http://dx.doi.org/10.1016/j.apenergy.2017.12.090.

[38] Jayasuriya L, Chaudry M, Qadrdan M, Wu J, Jenkins N. Energy hub modelling for multi-scale and multi-energy supply systems. In: 2019 IEEE Milan PowerTech. 2019, p. 1–6. http://dx.doi.org/10.1109/PTC.2019.8810641.

[39] Wang Y, Wang Y, Huang Y, Yang J, Ma Y, Yu H, et al. Operation optimization of regional integrated energy system based on the modeling of electricity-thermal-natural gas network. Appl Energy 2019;251:113410. http://dx.doi.org/10.1016/j.apenergy.2019.113410.

[40] Dolatabadi A, Mohammadi-ivatloo B, Abapour M, Tohidi S. Optimal stochastic design of wind integrated energy hub. IEEE Trans Ind Inf 2017;13(5):2379–88. http://dx.doi.org/10.1109/TII.2017.2664101.

[41] Najafi A, Falaghi H, Contreras J, Ramezani M. Medium-term energy hub management subject to electricity price and wind uncertainty. Appl Energy 2016;168:418–33. http://dx.doi.org/10.1016/j.apenergy.2016.01.074.

[42] Zare Oskouei M, Mohammadi-Ivatloo B, Abapour M, Shafiee M, Anvari-Moghaddam A. Techno-economic and environmental assessment of the coordinated operation of regional grid-connected energy hubs considering high penetration of wind power. J Cleaner Prod 2021;280:124275. http://dx.doi.org/10.1016/j.jclepro.2020.124275.

[43] Preston N, Maroufmashat A, Riaz H, Barbouti S, Mukherjee U, Tang P, et al. How can the integration of renewable energy and power-to-gas benefit industrial facilities? From techno-economic, policy, and environmental assessment. Int J Hydrogen Energy 2020;45(51):26559–73. http://dx.doi.org/10.1016/j.ijhydene.2020.07.040.

[44] Mohammadi M, Noorollahi Y, Mohammadi-ivatloo B, Hosseinzadeh M, Yousefi H, Khorasani ST. Optimal management of energy hubs and smart energy hubs – A review. Renew Sustain Energy Rev 2018;89:33–50. http://dx.doi.org/10.1016/j.rser.2018.02.035.

[45] Mohammadi M, Noorollahi Y, Mohammadi-ivatloo B, Yousefi H. Energy hub: From a model to a concept – A review. Renew Sustain Energy Rev 2017;80:1512–27. http://dx.doi.org/10.1016/j.rser.2017.07.030.

[46] Voldsund M. Exergy analysis of offshore oil and gas processing. 2014:155, NTNU-Trykk; 2014, URL: https://ntnuopen.ntnu.no/ntnu-xmlui/handle/11250/248017, [Accessed September 2021].

[47] Gunnerud V, Foss B, McKinnon K, Nygreen B. Oil production optimization solved by piecewise linearization in a Branch & Price framework. Comput Oper Res 2012;39(11):2469–77. http://dx.doi.org/10.1016/j.cor.2011.12.013.

[48] Tarhan B, Grossmann IE, Goel V. Stochastic programming approach for the planning of offshore oil or gas field infrastructure under decision-dependent uncertainty. Ind Eng Chem Res 2009;48(6):3078–97. http://dx.doi.org/10.1021/ie8013549.

[49] Mazzetti MJ, Nekså P, Walnum HT, Hemmingsen AKT. Energy-efficiency technologies for reduction of offshore CO2 emissions. Oil and Gas Facil 2014;3(01):89–96. http://dx.doi.org/10.2118/169811-PA.

[50] Looney B. Statistical review of world energy, 2020. 69, BP; 2020, p. 66, URL: https://www.bp.com/content/dam/bp/business-sites/en/global/corporate/pdfs/energy-economics/statistical-review/bp-stats-review-2020-full-report.pdf. [Accessed June 2021].

[51] Statistics Norway. Emissions to air. 2020, https://www.ssb.no/en/natur-og-miljo/forurensning-og-klima/statistikk/utslipp-til-luft. [Accessed May 2021].

[52] Ministry of Climate and Environment. Norway steps up 2030 climate goal to at least 50 % towards 55 %. 2020, https://www.regjeringen.no/en/aktuelt/norge-forsterker-klimamalet-for-2030-til-minst-50-prosent-og-opp-mot-55-prosent/id2689679/. [Accessed June 2021].

[53] Sean Bray. Carbon taxes in europe. 2022, "https://taxfoundation.org/carbon-taxes-in-europe-2022/".[Accessed June 2022].

[54] Norwegian Petroleum Directorate. Emissions to air. 2020, https://www.norskpetroleum.no/en/environment-and-technology/emissions-to-air/. [Accessed June 2022].

[55] Equinor. Reducing our greenhouse gas emissions. 2021, https://www.equinor.com/en/news/2020-01-06-climate-ambitions-norway.html. [Accessed July 2021].

[56] Vår-Energi. Sustainability report. 2019, https://varenergi.no/wp-content/uploads/2020/06/V%C3%A5r-Energi-Sustainability-Report-2019.pdf. [Accessed July 2021].

[57] Bergmo PES, Grimstad A-A. Water shutoff technologies for reduced energy consumption. In: SPE Norway Subsurface Conference. 2022, http://dx.doi.org/10.2118/209555-MS.

[58] Lindegaard A, Aasrud A, Andersen A, Andresen SR, Asphjell T, Backer EB, et al. Kunnskapsgrunnlag for lavutslippsutvikling. Miljødirektoratet; 2014, URL: https://www.miljodirektoratet.no/publikasjoner/2014/oktober-2014/kunnskapsgrunnlag-for-lavutslippsutvikling/. [Accessed June 2021].

[59] Norwegian Petroleum Directorate. Norsk petroleum. 2020, https://www.norskpetroleum.no/en/. [Accessed May 2021].

[60] Riboldi L, Nord LO. Concepts for lifetime efficient supply of power and heat to offshore installations in the North Sea. Energy Convers Manage 2017;148:860–75. http://dx.doi.org/10.1016/j.enconman.2017.06.048.

[61] Directorate NP. Power from land report. Norwegian Petroleum Directorate; 2020, URL: https://www.npd.no/fakta/publikasjoner/rapporter/rapportarkiv/kraft-fra-land-til-norsk-sokkel/. [Accessed June 2021].

[62] Equinor. Hywind Tampen: the world's first renewable power for offshore oil and gas. 2020.

[63] Svendsen HG, Hadiya M, Øyslebø EV, Uhlen K. Integration of offshore wind farm with multiple oil and gas platforms. In: 2011 IEEE Trondheim PowerTech. IEEE; 2011, p. 1–3. http://dx.doi.org/10.1109/PTC.2011.6019309.

[64] He W, Jacobsen G, Anderson T, Olsen F, Hanson TD, Korpås M, et al. The potential of integrating wind power with offshore oil and gas platforms. Wind Eng 2010;34(2):125–37. http://dx.doi.org/10.1260/0309-524X.34.2.125.

[65] Marvik JI, Øyslebø EV, Korpås M. Electrification of offshore petroleum installations with offshore wind integration. Renew Energy 2013;50:558–64. http://dx.doi.org/10.1016/j.renene.2012.07.010.

[66] Trötscher T, Korpås M. A framework to determine optimal offshore grid structures for wind power integration and power exchange. Wind Energy 2011;14:977–92. http://dx.doi.org/10.1002/we.461.

[67] Svendsen HG. Planning tool for clustering and optimised grid connection of offshore wind farms. Energy Procedia 2013;35:297–306. http://dx.doi.org/10.1016/j.egypro.2013.07.182.

[68] Foss B, Knudsen BR, Grimstad B. Petroleum production optimization – a static or dynamic problem? Comput Chem Eng 2018;114:245–53. http://dx.doi.org/10.1016/j.compchemeng.2017.10.009.

[69] Backe S, Ahang M, Tomasgard A. Stable stochastic capacity expansion with variable renewables: Comparing moment matching and stratified scenario generation sampling. Appl Energy 2021;302:117538. http://dx.doi.org/10.1016/j.apenergy.2021.117538.

[70] Kaut M, Midthun KT, Werner AS, Tomasgard A, Hellemo L, Fodstad M. Multi-horizon stochastic programming. Comput Manag Sci 2014;11(1–2):179–93. http://dx.doi.org/10.1007/s10287-013-0182-6.

[71] van der Heijde B, Vandermeulen A, Salenbien R, Helsen L. Representative days selection for district energy system optimisation: a solar district heating system with seasonal storage. Appl Energy 2019;248:79–94. http://dx.doi.org/10.1016/j.apenergy.2019.04.030.

[72] Mazzi N, Grothey A, McKinnon K, Sugishita N. Benders decomposition with adaptive oracles for large scale optimization. Math Program Comput 2020;12:1–21. http://dx.doi.org/10.1007/s12532-020-00197-0.

[73] Norwegian Petroleum Directorate. Open data. 2022, https://www.npd.no/en/about-us/information-services/open-data/. [Accessed March 2022].

[74] Zhang H. REORIENT (Public). 2021, http://dx.doi.org/10.5281/zenodo.6665527.

[75] Norwegian Oil and Gas Association. Norsk olje & gass - enviornment. 2021, https://www.norskoljeoggass.no/miljo/miljorapporter/miljorapport-2021/feltspesifikke-utslippsrapporter/. [Accessed May 2021].

[76] Norwegian Petroleum Directorate. The norwegian national data repository for petroleum data. 2021, https://www.npd.no/en/diskos/. [Accessed June 2021].

[77] The LowEmission Research Centre. SINTEF. 2020, https://www.sintef.no/projectweb/lowemission/. [Accessed May 2021].

[78] Dunning I, Huchette J, Lubin M. JuMP: A modeling language for mathematical optimization. SIAM Rev 2017;59(2):295–320. http://dx.doi.org/10.1137/15M1020575.

[79] Gurobi Optimization LLC. Gurobi optimizer reference manual. 2021, "https://www.gurobi.com". [Accessed May 2021].

[80] Nguyen T-V, Jacyno T, Breuhaus P, Voldsund M, Elmegaard B. Thermodynamic analysis of an upstream petroleum plant operated on a mature field. Energy 2014;68:454–69. http://dx.doi.org/10.1016/j.energy.2014.02.040.

[81] Statistics Norway. Electricity. 2020, https://www.ssb.no/en/energi-og-industri/energi/statistikk/elektrisitet. [Accessed May 2021].

[82] Birge JR, Louveaux F. Introduction To Stochastic Programming. Springer Science & Business Media; 2011, http://dx.doi.org/10.1007/978-1-4614-0237-4.

[83] Svendsen HG. Optimised operation of low-emission offshore oil and gas platform integrated energy systems. 2022, arXiv:10.48550/ARXIV.2202.05072.